Polarization Observables in Vector Meson Photoproduction from the FROST Experiment using CLAS at Jefferson Lab

Priyashree Roy

Florida State University/University of Michigan

User Group Meeting

Jefferson Lab, Virginia

June 21, 2017

Outline

Outline

Baryon Spectroscopy

Open question in the non-perturbative regime (where QCD is difficult to solve): How does QCD give rise to excited baryons?

- What is the origin of confinement? How are confinement and chiral symmetry breaking connected?
- What are the relevant degrees of freedom? How do they evolve with energy?

Baryon Spectroscopy

Open question in the non-perturbative regime (where QCD is difficult to solve): How does QCD give rise to excited baryons?

- What is the origin of confinement? How are confinement and chiral symmetry breaking connected?
- What are the relevant degrees of freedom? How do they evolve with energy?

Baryon Spectroscopy

Open question in the non-perturbative regime (where QCD is difficult to solve): How does QCD give rise to excited baryons?

- What is the origin of confinement? How are confinement and chiral symmetry breaking connected?
- What are the relevant degrees of freedom? How do they evolve with energy?

Light Baryon Spectroscopy

Effective degrees of freedom

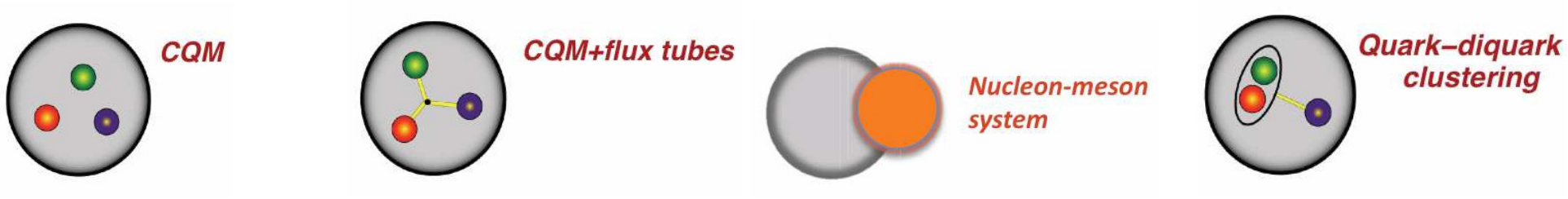

+ Lattice-QCD computations
(complementary to phenomenological models)

Light Baryon Spectroscopy: Map out the excited states of light baryons, identify the underlying multiplets to reveal answers to the open questions.

Understanding the Light Baryon Spectrum

- **Underlying Pattern**: the resonances can be grouped into bands and multiplets.
- The level counting in LQCD for each J^P in each band is **consistent** with CQM.

A CQM prediction for N*

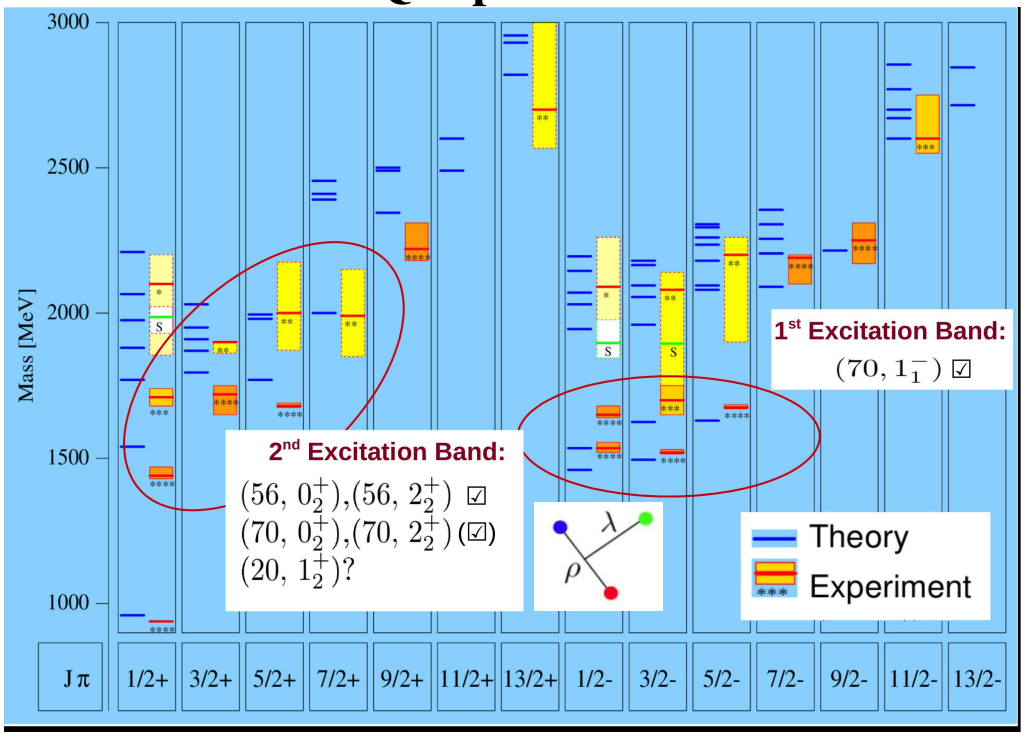

S. Capstick and N. Isgur, Phys. Rev. D **34** (1986) 2809

N* from Lattice-QCD

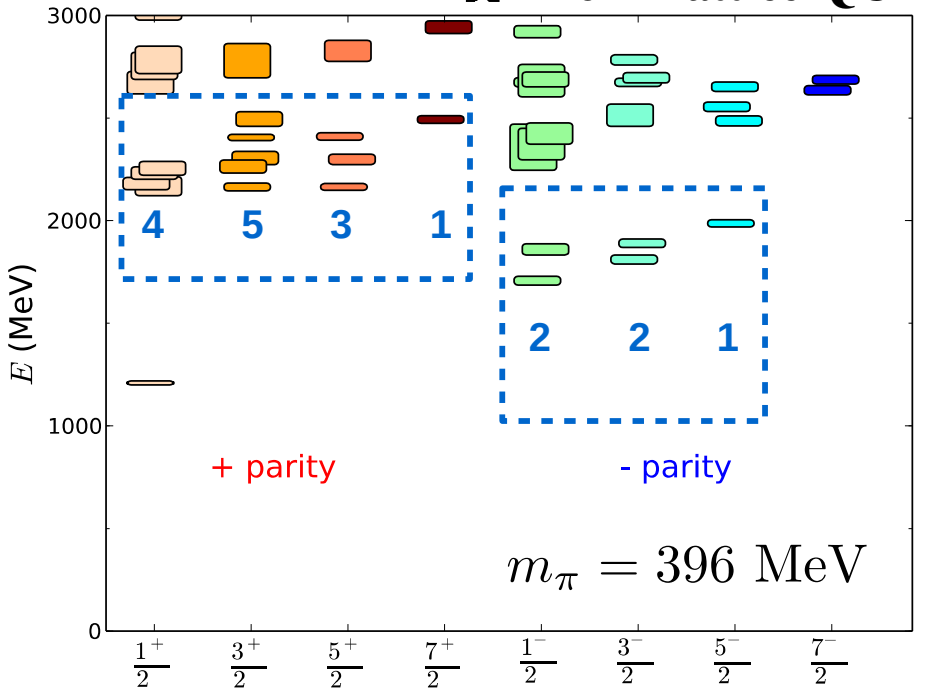

R. Edwards *et al.* Phys. Rev. D **84** 074508 (2011)
Picture courtesy V. Bukert (CLAS collaboration meeting 2015)

Understanding the Light Baryon Spectrum

- The quartet of (**70**, 2_2^+) requires both oscillators to be excited: inconsistent with the static quark-diquark picture.
- No sign of 'freezing' in LQCD calculations.

A CQM prediction for N*

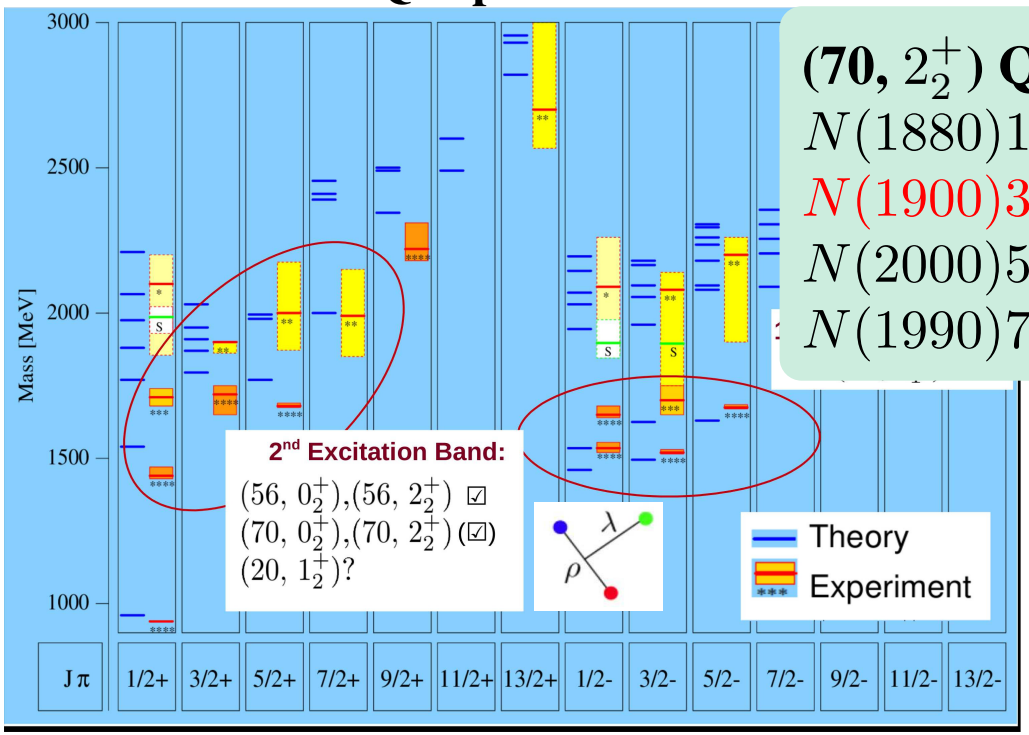

(70, 2_2^+) Quartet

$N(1880)1/2^+$ **

$N(1900)3/2^+$ ***

$N(2000)5/2^+$ **

$N(1990)7/2^+$ **

N* from Lattice-QCD

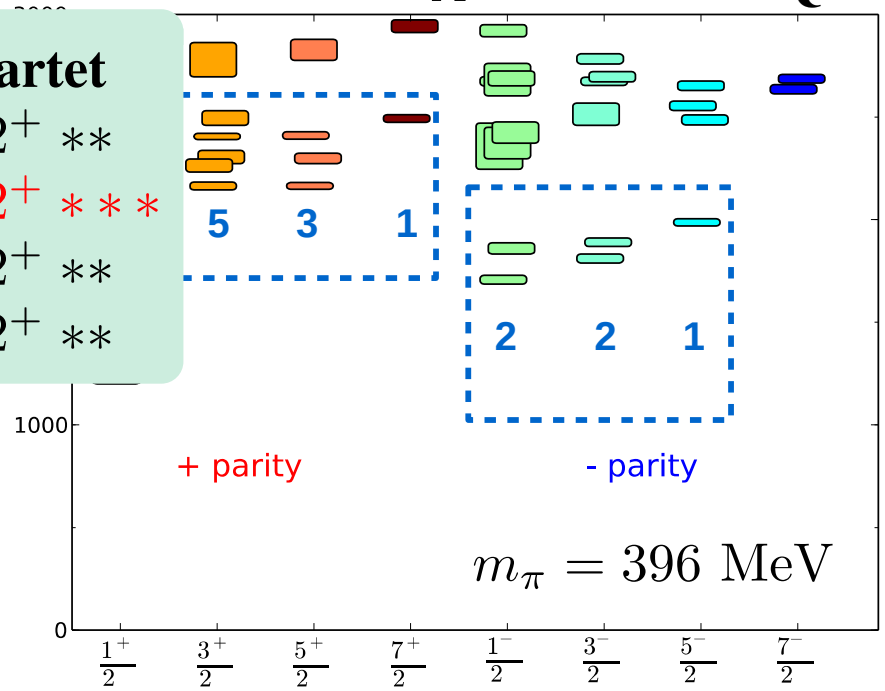

Bradford *et al.* (CLAS), PRC **75**, 035205 (2007), Observables C_x, C_z from $\vec{\gamma}p \to K^+\vec{\Lambda}$
Fits: BnGa Model, V.A. Nikonov *et al.*, Phy. Lett. B **662**, 245 (2008)

Understanding the Light Baryon Spectrum

Baryon spectrum not well understood, particularly above 1.7 GeV in W.

A CQM prediction for N*

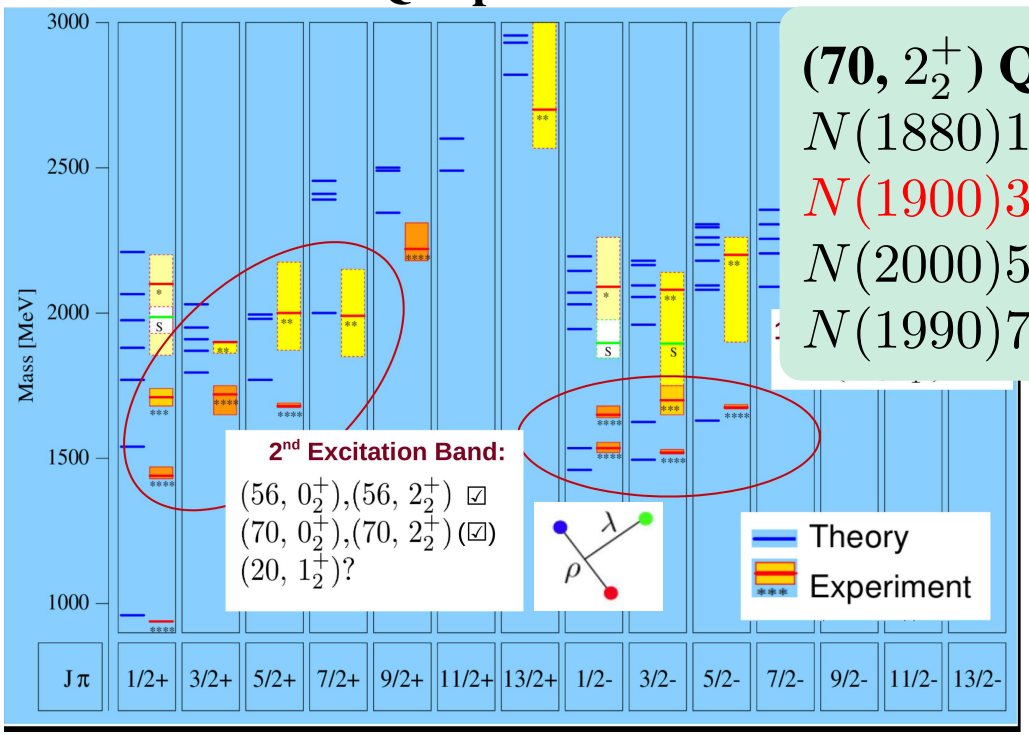

(70, 2_2^+) Quartet

$N(1880)1/2^+$ **

$N(1900)3/2^+$ ***

$N(2000)5/2^+$ **

$N(1990)7/2^+$ **

N* from Lattice-QCD

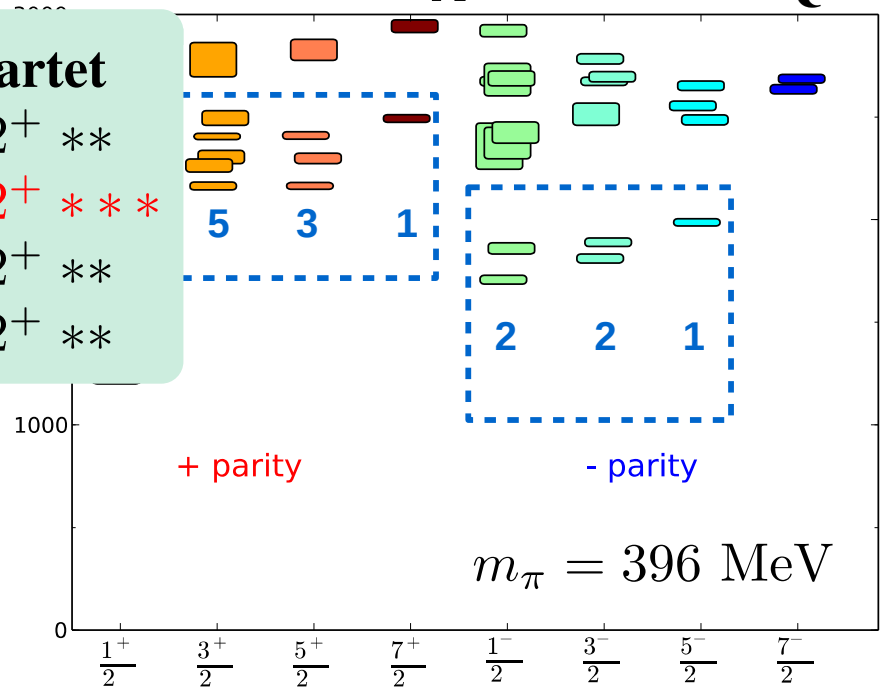

Bradford *et al.* (CLAS), PRC **75**, 035205 (2007), Observables C_x, C_z from $\vec{\gamma}p \to K^+\vec{\Lambda}$
Fits: BnGa Model, V.A. Nikonov *et al.*, Phy. Lett. B **662**, 245 (2008)

Vector Meson and Multi-Pion Photoproduction

Studying these photoproduction reactions will aid in a better understanding of the spectrum:

- Further investigation of poorly-understood properties of many known resonances: N^* contributions to these reactions have mostly remained under-explored.

		Status as seen in								
Particle J^P	overall	$N\gamma$	$N\pi$	$N\eta$	$N\sigma$	$N\omega$	ΛK	ΣK	$N\rho$	$\Delta\pi$
$N(1700)\,3/2^-$	***	**	***	*			*	*	*	***
$N(1710)\,1/2^+$	****	****	****	***		**	****	**	*	**
$N(1720)\,3/2^+$	****	****	****	***			**	**	**	*
$N(1860)\,5/2^+$	**		**						*	*
$N(1875)\,3/2^-$	***	***	*			**	***	**		***
$N(1880)\,1/2^+$	**	*	*		**		*			
$N(1895)\,1/2^-$	**	**	*	**			**	*		
$N(1900)\,3/2^+$	***	***	**	**		**	***	**	*	**
$N(1990)\,7/2^+$	**	**	**					*		
$N(2000)\,5/2^+$	**	**	*	**			**	*	**	
$N(2040)\,3/2^+$	*		*							
$N(2060)\,5/2^-$	**	**	**	*				**		
$N(2100)\,1/2^+$	*		*							
$N(2120)\,3/2^-$	**	**	**				*	*		
$N(2190)\,7/2^-$	****	***	****			*	**		*	
$N(2220)\,9/2^+$	****		****							
$N(2250)\,9/2^-$	****		****							
$N(2300)\,1/2^+$	**		**							
$N(2570)\,5/2^-$	**		**							

Particle Data Group 2017

Vector Meson and Multi-Pion Photoproduction

Studying these photoproduction reactions will aid in a better understanding of the spectrum:

- Further investigation of poorly-understood properties of many known resonances: N^* contributions to these reactions have mostly remained under-explored.
- High-mass resonances preferably decay to heavier mesons, e.g. vector mesons (e.g. ω, ρ, ϕ), or sequentially decay to multi-particle final states via intermediate resonances.

		Status as seen in								
Particle J^P	overall	$N\gamma$	$N\pi$	$N\eta$	$N\sigma$	$N\omega$	ΛK	ΣK	$N\rho$	$\Delta\pi$
$N(1700)\,3/2^-$	***	**	***	*			*	*	*	***
$N(1710)\,1/2^+$	****	****	****	***		**	****	**	*	**
$N(1720)\,3/2^+$	****	****	****	***			**	**	**	*
$N(1860)\,5/2^+$	**		**						*	*
$N(1875)\,3/2^-$	***	***	*			**	***	**		***
$N(1880)\,1/2^+$	**	*	*		**		*			
$N(1895)\,1/2^-$	**	**	*	**			**	*		
$N(1900)\,3/2^+$	***	***	**	**		**	***	**	*	**
$N(1990)\,7/2^+$	**	**	**					*		
$N(2000)\,5/2^+$	**	**	*	**			**	*	**	
$N(2040)\,3/2^+$	*		*							
$N(2060)\,5/2^-$	**	**	**	*				**		
$N(2100)\,1/2^+$	*		*							
$N(2120)\,3/2^-$	**	**	**				*	*		
$N(2190)\,7/2^-$	****	***	****			*	**		*	
$N(2220)\,9/2^+$	****		****							
$N(2250)\,9/2^-$	****		****							
$N(2300)\,1/2^+$	**		**							
$N(2570)\,5/2^-$	**		**							

Particle Data Group 2017

Vector Meson and Multi-Pion Photoproduction

Studying these photoproduction reactions will aid in a better understanding of the spectrum:

- Further investigation of poorly-understood properties of many known resonances: N^* contributions to these reactions have mostly remained under-explored.
- High-mass resonances preferably decay to heavier mesons, e.g. vector mesons (e.g. ω, ρ, ϕ), or sequentially decay to multi-particle final states via intermediate resonances.
- These factors motivated the analysis of $\gamma p \to p\omega \to p\pi^+\pi^-(\pi^0)$ and $\gamma p \to p\pi^+\pi^-$ reactions. The latter gives information on $N^* \to p\rho$, and on sequential decays via intermediate resonances.

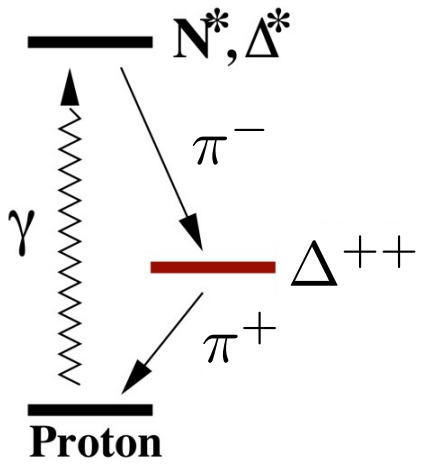

Sequential decays in $\gamma\, p \;\to\; p\,\pi\,\pi$

Why are Spin Observables Important?

w/o polarizer

w/ polarizer

Polarized measurements in addition to the unpolarized cross section measurements necessary to disentangle and reveal the resonances with minimum ambiguities.

Why are Spin Observables Important?

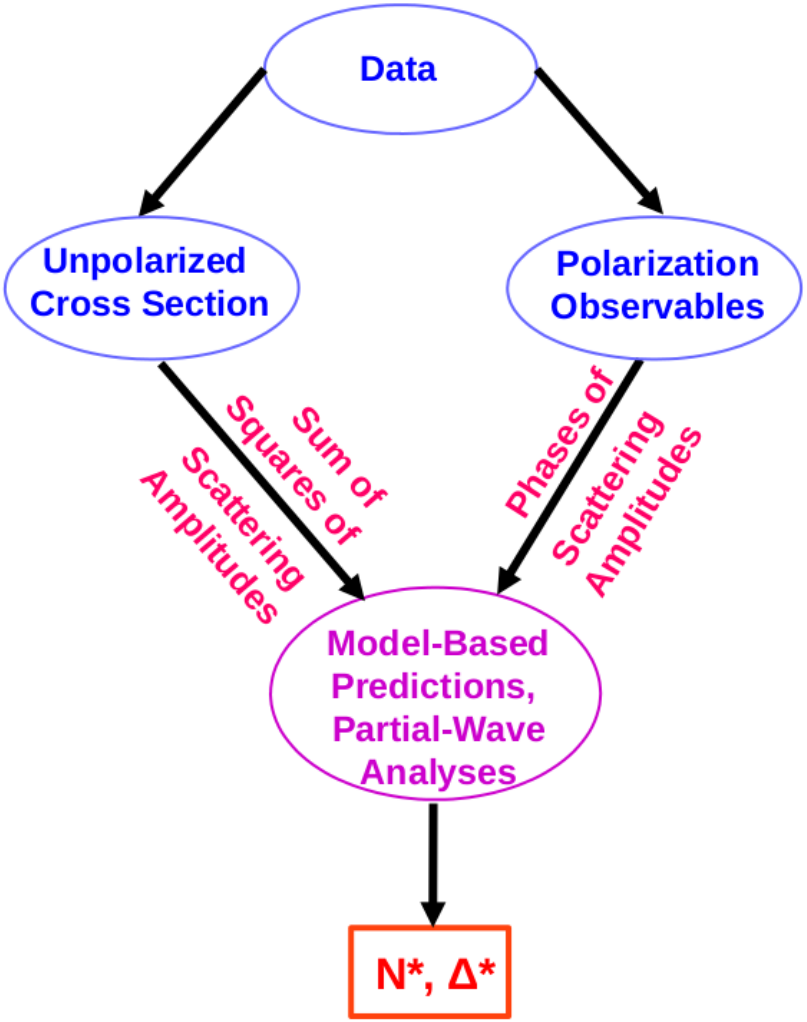

w/o polarizer

w/ polarizer

Polarized measurements in addition to the unpolarized cross section measurements necessary to disentangle and reveal the resonances with minimum ambiguities.

Spin Observables for $\vec{\gamma}\vec{p} \to p\pi^+\pi^-$ & $p\omega$ @ CLAS

The FROST N^* Program in Hall B, JLab

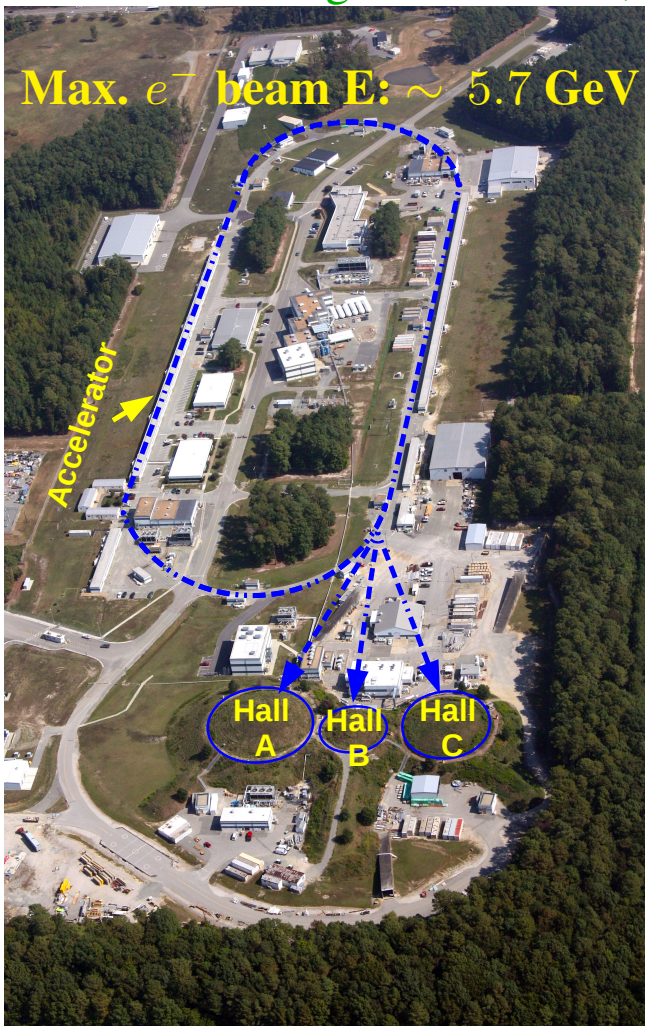

$\vec{\gamma}\vec{p} \to p\omega$

Beam \ Target	Transversely Pol.	Longitudinally Pol.
Linearly Pol.	Σ, T, H, P	Σ, G
Circularly Pol.	F, T	E

$\vec{\gamma}\vec{p} \to p\pi^+\pi^-$

Beam \ Target	Transversely Pol.	Longitudinally Pol.
Linearly Pol.	$P^{s,c}_{x,y}$, $P_{x,y}$, $I^{s,c}$	$P^{s,c}_{z}$, P_{z}, $I^{s,c}$
Circularly Pol.	$P^{\odot}_{x,y}$, $P_{x,y}$, $I^{\odot}$	$P^{\odot}_{z}$, P_{z}, $I^{\odot}$

13 spin observables extracted in my analysis

Data acquired

Final or prelim. results available

The FROST Experiment using CLAS at JLab

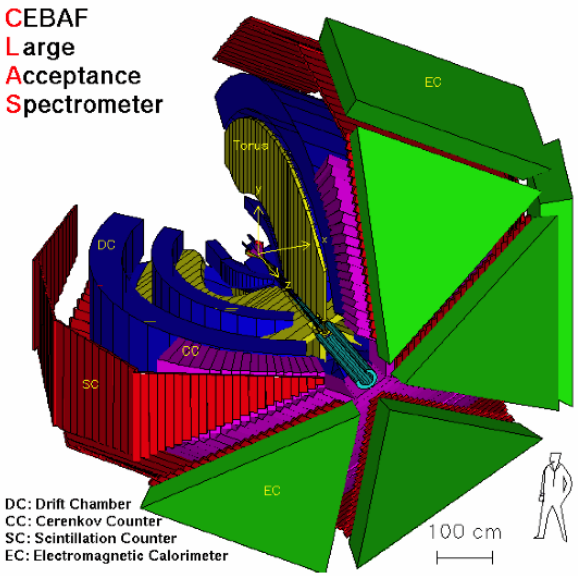

large acceptance for charged particles, well-suited for spectroscopy.

Coherent edges: 0.9-2.1 GeV (0.2 GeV wide)
Deg. of linear beam pol., δ_γ: $40 - 60\%$

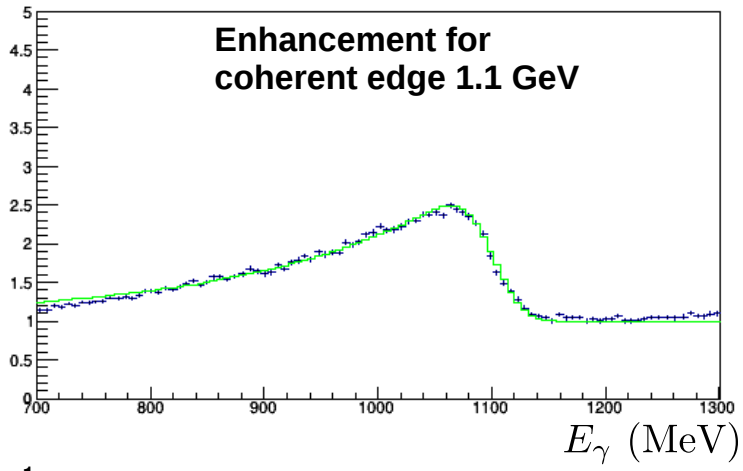

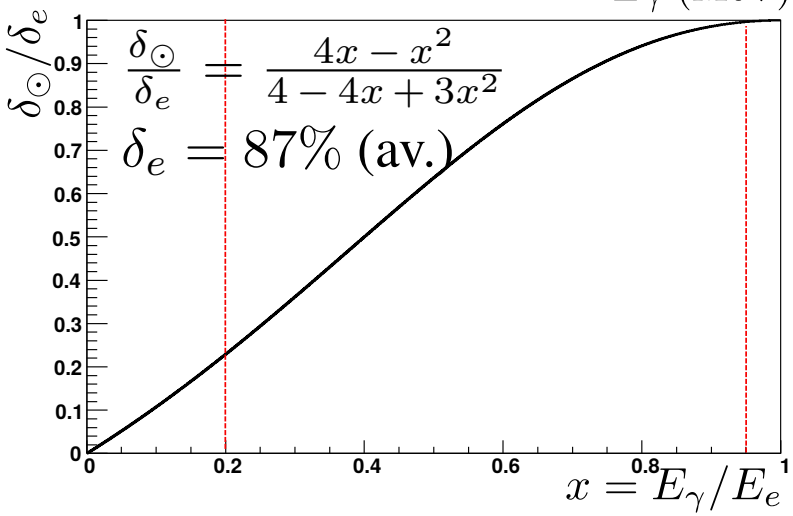

g9b run (Mar to Aug, 2010)

Photon Pol.: Linear/Circular

Target: (Nitroxyl) Doped Butanol (C_4H_9OH)

Target Pol.: Transverse

W **range:** 1.4-2.1 GeV (Lin. Data)
1.5-2.5 GeV (Circ. Data)

The FROzen Spin Target (FROST) Apparatus

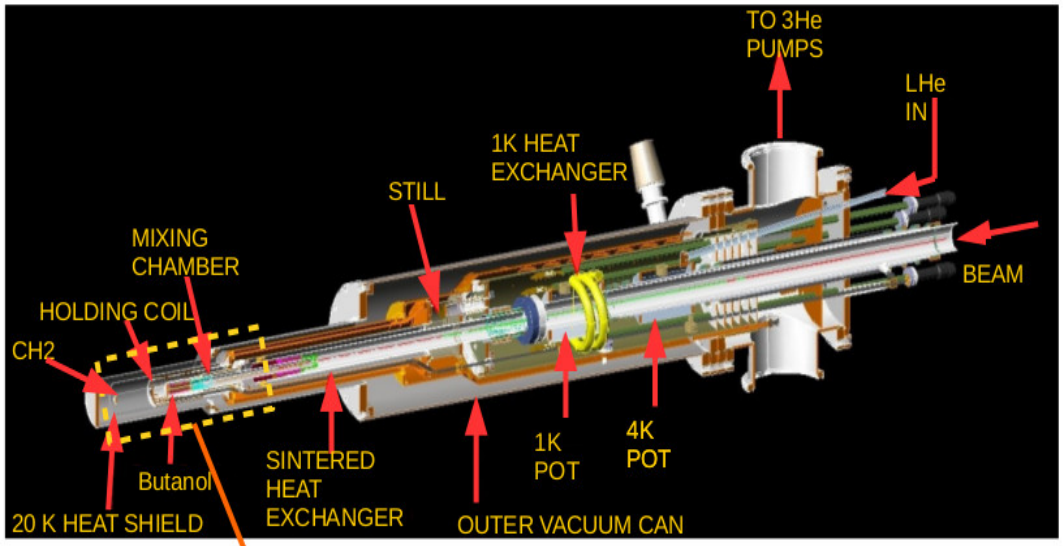

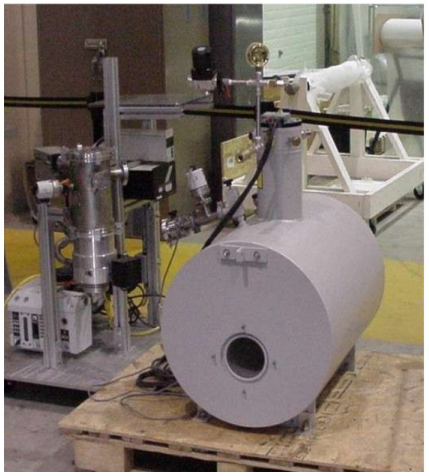

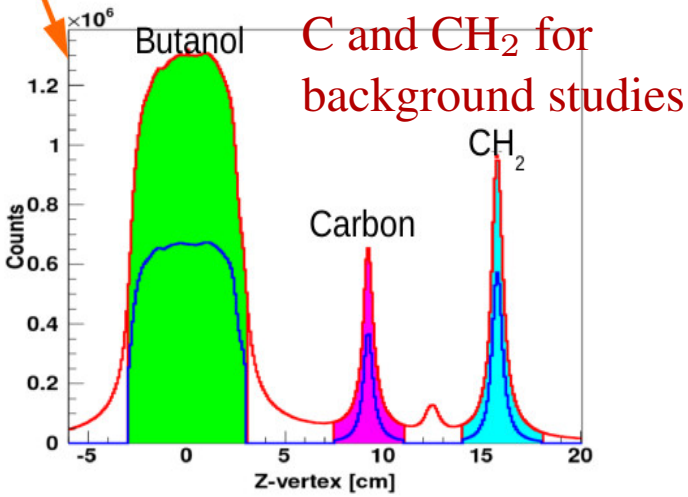

- Polarizing field = 5 T, T$\sim$ 0.3 K
- Dipole holding field = 0.5 T, T$\sim$ 50 mK
- Offset angle = 116.1 $\pm$ 0.4° from x_{lab}
- Av. target pol. = 81.0 $\pm$ 1.7%
- Relaxation time: 3400 hrs w/ beam, 4000 hrs w/o beam

Outline

Data Selection and Analysis

- **Topology for $p\omega$ (89% branching fraction):**
  $\vec{\gamma}\vec{p} \rightarrow p\pi^+\pi^-$(missing π^0)
  Topology identified using Kinematic fitting.
- **Topologies for $p\pi^+\pi^-$:**
  $\vec{\gamma}\vec{p} \rightarrow p\pi^+$ (missing π^-)
  $\vec{\gamma}\vec{p} \rightarrow p\pi^-$ (missing π^+)
  $\vec{\gamma}\vec{p} \rightarrow p\pi^+\pi^-$ (no missing particle)
  The observables are weighted avg. over topologies.
- **Standard cuts & corrections:** vertex cut, photon selection, β cuts, E-p corrections.
- **Event-based method**[1] for signal-background separation.
- **Event-based maximum likelihood method**[2] to fit angular distributions in $\phi_{\text{lab}}^{\text{recoil}}$ and extract the polarization observables.

Data Selection and Analysis

- **Topology for $p\omega$ (89% branching fraction):**
  $\vec{\gamma}\vec{p} \rightarrow p\pi^+\pi^-$(missing π^0)
  Topology identified using Kinematic fitting.
- **Topologies for $p\pi^+\pi^-$:**
  $\vec{\gamma}\vec{p} \rightarrow p\pi^+$ (missing π^-)
  $\vec{\gamma}\vec{p} \rightarrow p\pi^-$ (missing π^+)
  $\vec{\gamma}\vec{p} \rightarrow p\pi^+\pi^-$ (no missing particle)
  The observables are weighted avg. over topologies.
- **Standard cuts & corrections:** vertex cut, photon selection, β cuts, E-p corrections.
- **Event-based method**[1] for signal-background separation.
- **Event-based maximum likelihood method**[2] to fit angular distributions in $\phi_{\text{lab}}^{\text{recoil}}$ and extract the polarization observables.

Data Selection and Analysis

- **Topology for $p\omega$ (89% branching fraction):**
  $\vec{\gamma}\vec{p} \rightarrow p\pi^+\pi^-(\text{missing } \pi^0)$
  Topology identified using Kinematic fitting.
- **Topologies for $p\pi^+\pi^-$:**
  $\vec{\gamma}\vec{p} \rightarrow p\pi^+$ (missing π^-)
  $\vec{\gamma}\vec{p} \rightarrow p\pi^-$ (missing π^+)
  $\vec{\gamma}\vec{p} \rightarrow p\pi^+\pi^-$ (no missing particle)
  The observables are weighted avg. over topologies.
- **Standard cuts & corrections:** vertex cut, photon selection, β cuts, E-p corrections.
- **Event-based method**[1] for signal-background separation.
- **Event-based maximum likelihood method**[2] to fit angular distributions in $\phi_{\text{lab}}^{\text{recoil}}$ and extract the polarization observables.

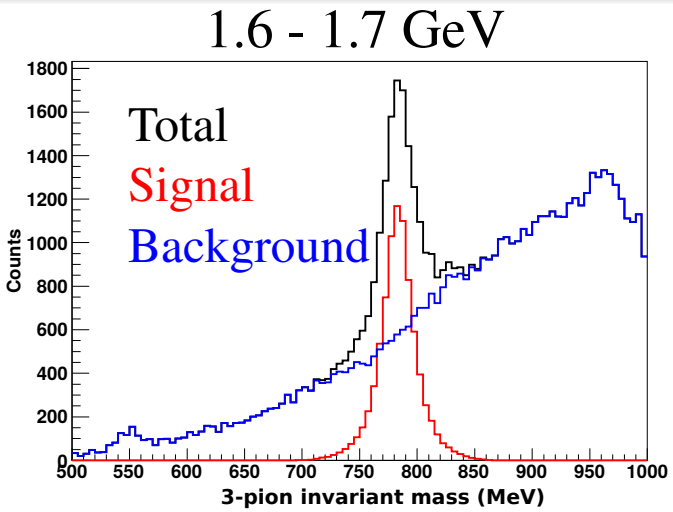

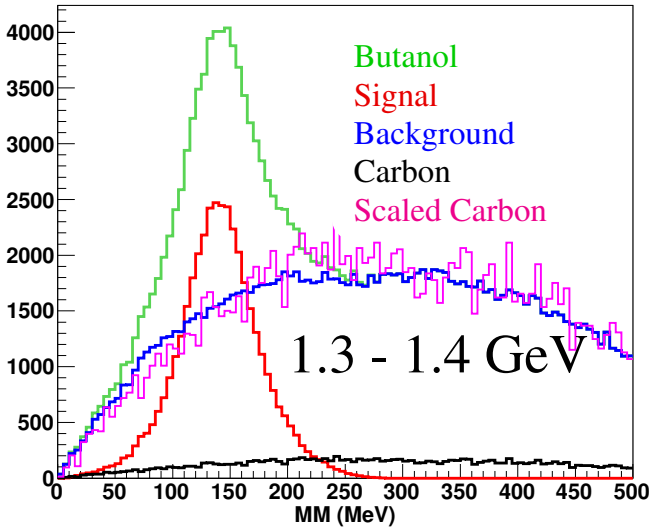

[1] M. Williams *et al.*, JINST 4 (2009) P10003

Data Selection and Analysis

- **Topology for $p\omega$ (89% branching fraction):**
  $\vec{\gamma}\vec{p} \rightarrow p\pi^+\pi^-(\text{missing } \pi^0)$
  Topology identified using Kinematic fitting.
- **Topologies for $p\pi^+\pi^-$:**
  $\vec{\gamma}\vec{p} \rightarrow p\pi^+$ (missing π^-)
  $\vec{\gamma}\vec{p} \rightarrow p\pi^-$ (missing π^+)
  $\vec{\gamma}\vec{p} \rightarrow p\pi^+\pi^-$ (no missing particle)
  The observables are weighted avg. over topologies.
- **Standard cuts & corrections:** vertex cut, photon selection, β cuts, E-p corrections.
- **Event-based method**[1] for signal-background separation.
- **Event-based maximum likelihood method**[2] to fit angular distributions in $\phi_{\text{lab}}^{\text{recoil}}$ and extract the polarization observables.

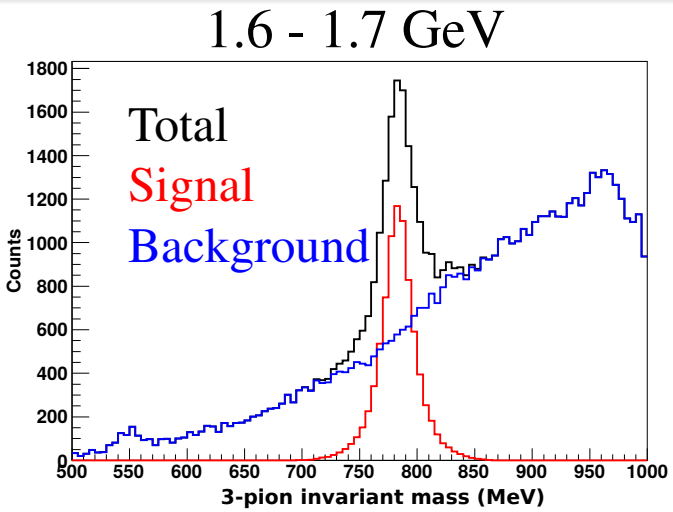

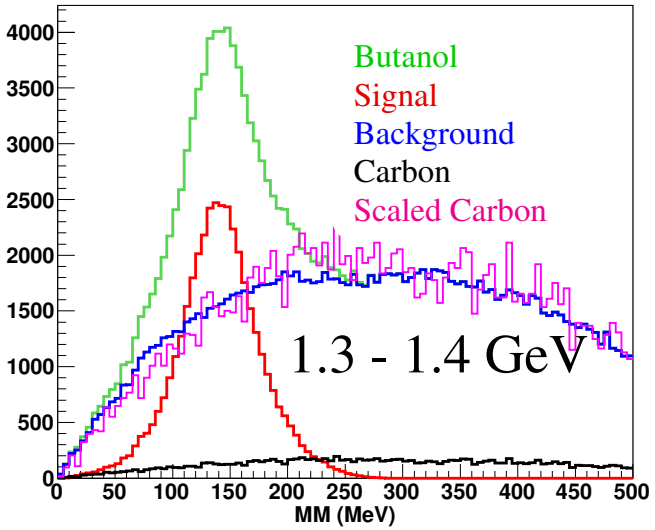

[1] M. Williams *et al.*, JINST 4 (2009) P10003
[2] D G Ireland, CLAS Note 2011-010

Results

Results in $\vec{\gamma}\vec{p} \rightarrow p\omega$

Published Results in $\gamma p \rightarrow p\omega$

Isospin filter (sensitive to N^* only), reduces complexity

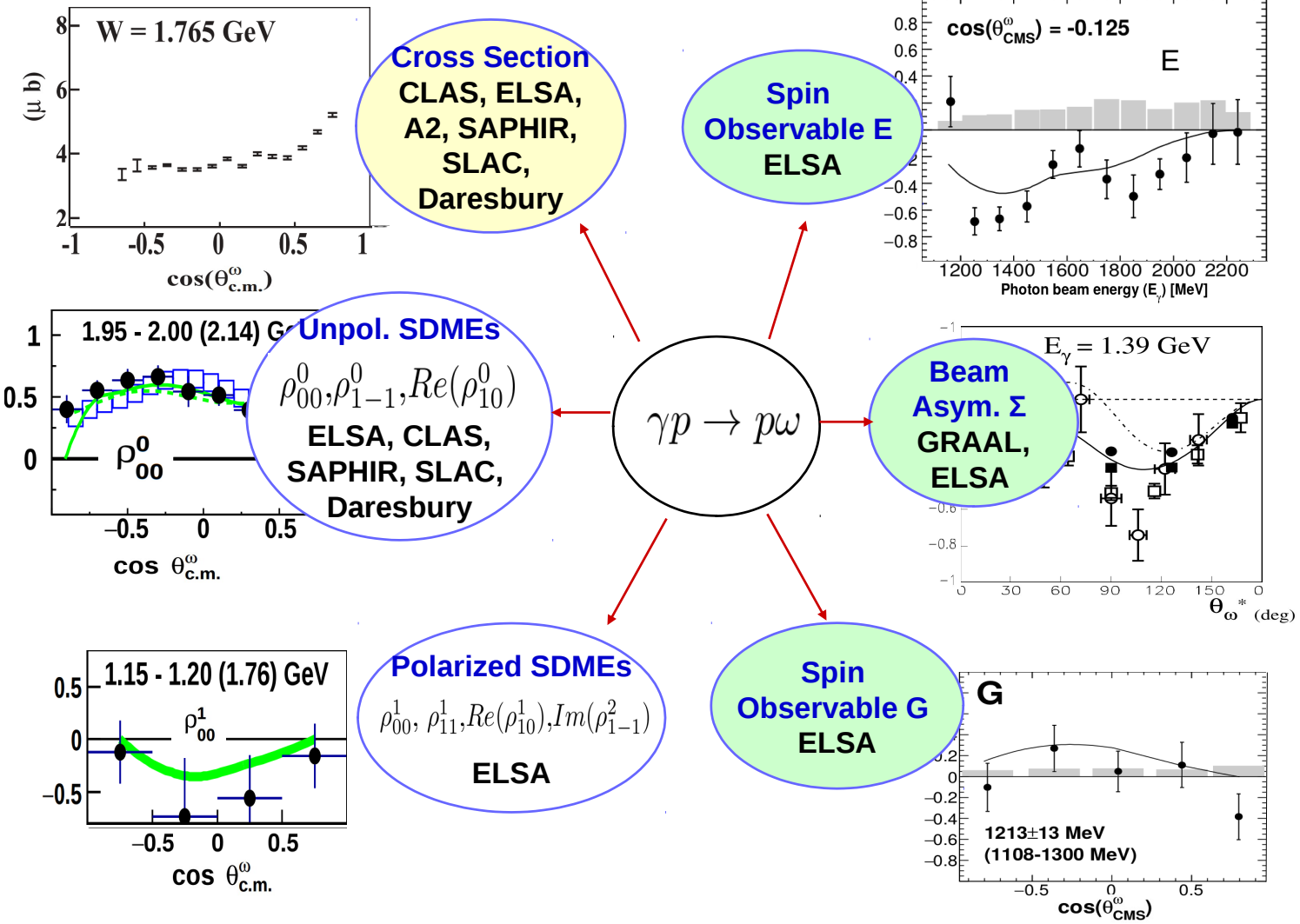

Published Results + New Spin Observables from FROST

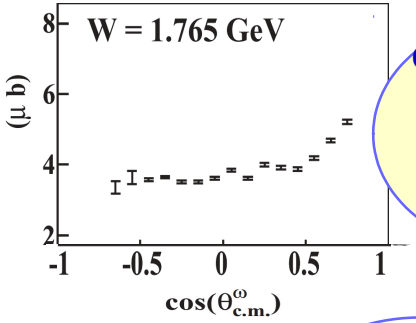

Cross Section
CLAS, ELSA, A2, SAPHIR, SLAC, Daresbury

Spin Observable E
ELSA

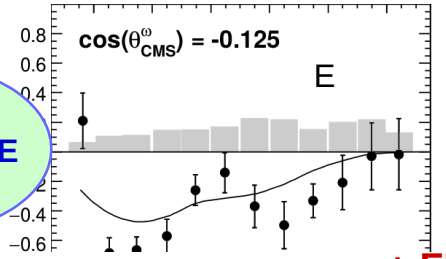

+ FROST (Prelim.) Results

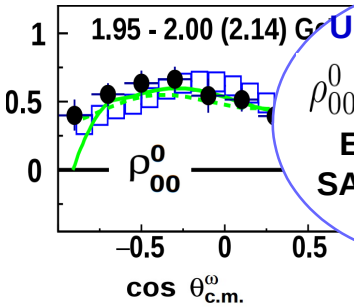

Unpol. SDMEs
$\rho^0_{00}, \rho^0_{1-1}, Re(\rho^0_{10})$
ELSA, CLAS, SAPHIR, SLAC, Daresbury

γp

Beam \ Target	Transversely Pol.	Longitudinally Pol.
Linearly Pol.	Σ, T, H, P	Σ, G
Circularly Pol.	F, T	E

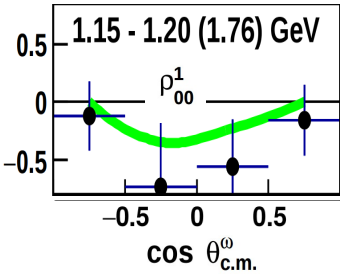

Polarized SDMEs
$\rho^1_{00}, \rho^1_{11}, Re(\rho^1_{10}), Im(\rho^2_{1-1})$
ELSA

Spin Observable G
ELSA

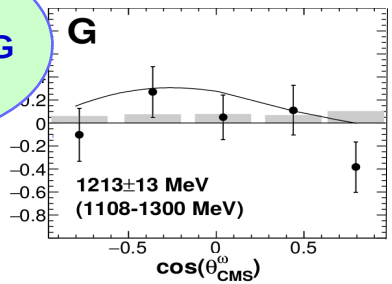

Importance of the Spin Observables from FROST

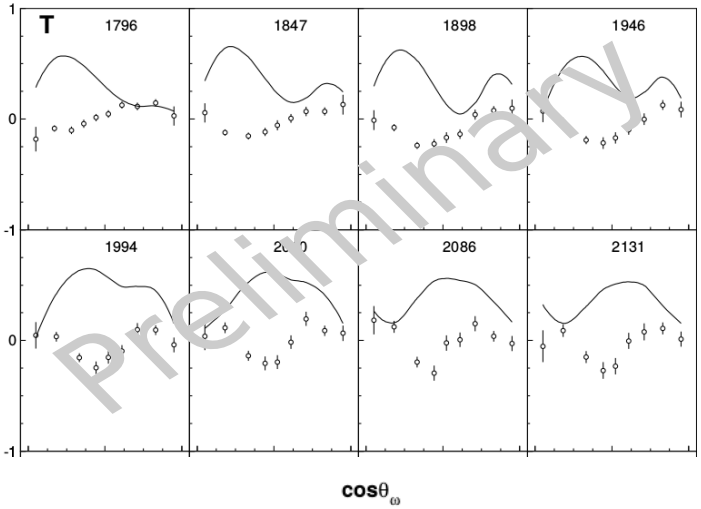

- BnGa-2016 solution, based on fits to ELSA data + new high statistics Σ from CLAS-g8b, was not entirely unique. Other acceptable solutions existed.
- BnGa-2016 predictions did NOT describe the new FROST observables well.
- Adding the new FROST observables to BnGa database has reduced ambiguities : BnGa-2017 PWA solution

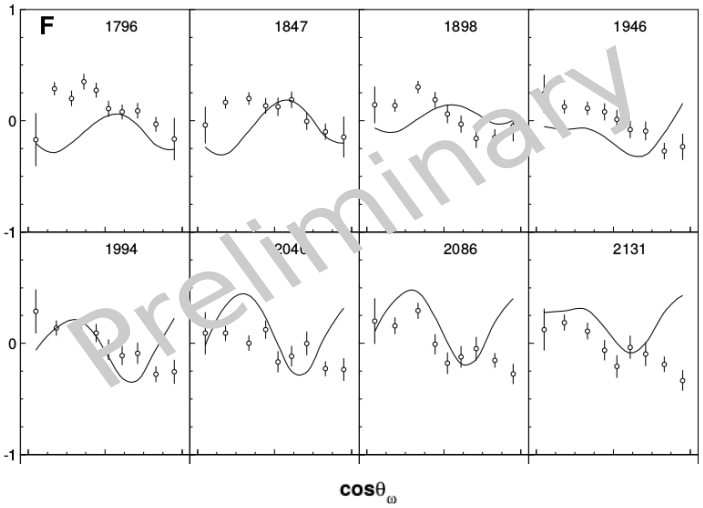

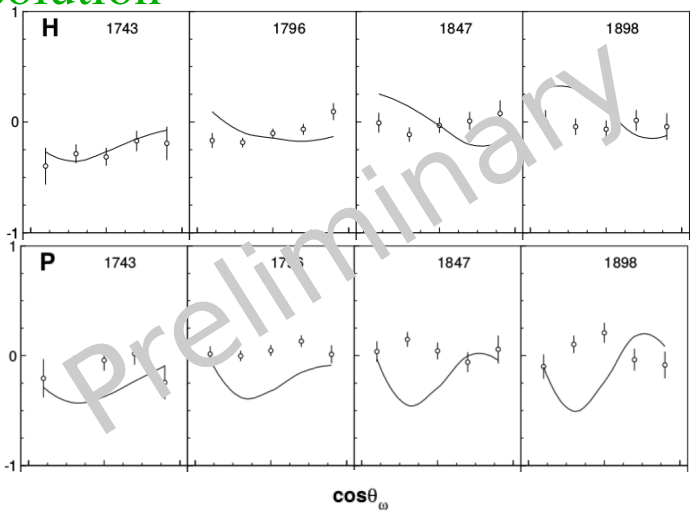

Beam Asymmetry Σ in $\vec{\gamma}p \to p\omega$

P. Roy *et al.* (CLAS-FROST), paper under review

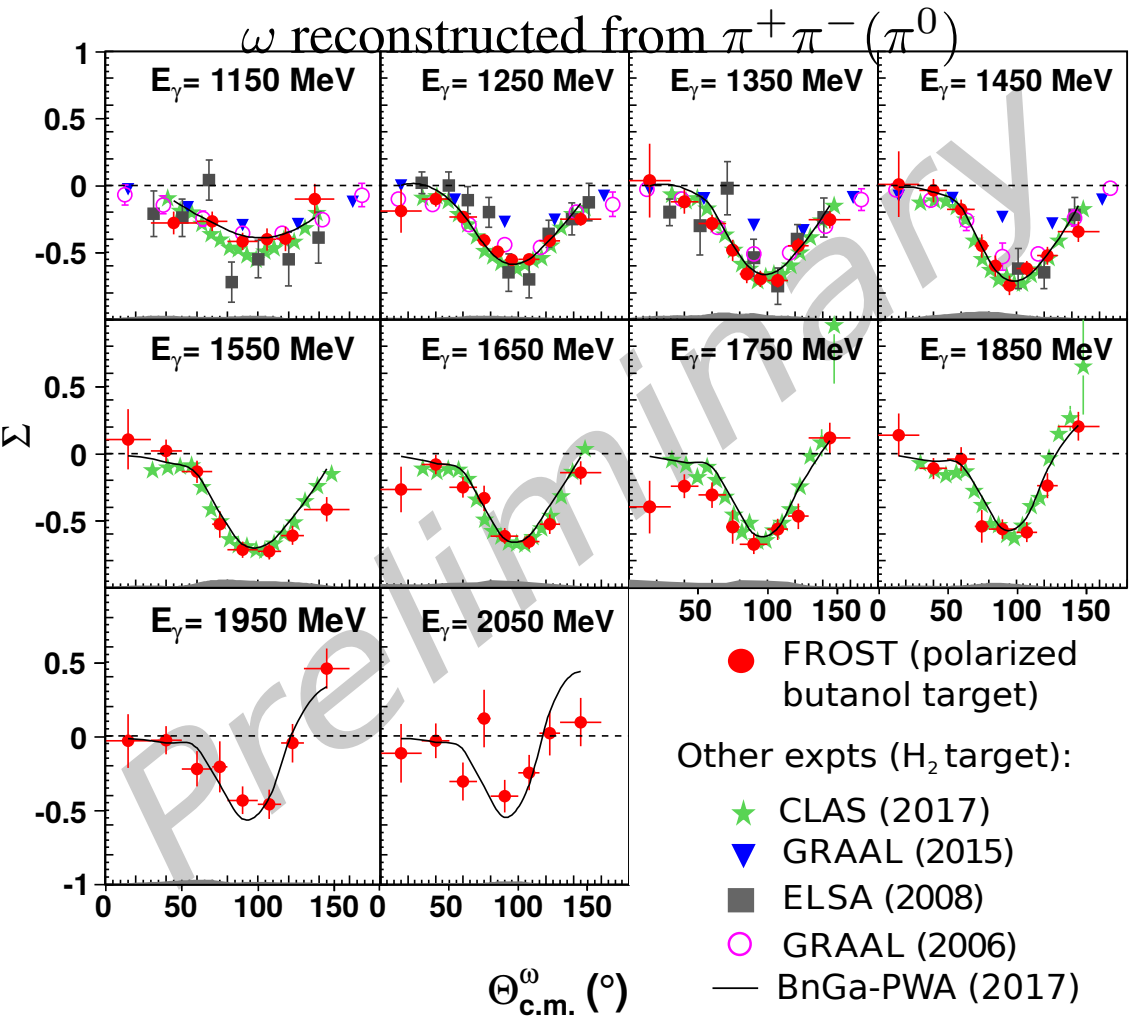

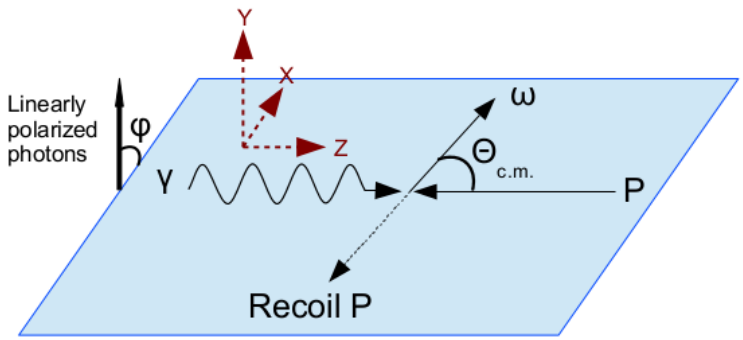

$$\sigma = \sigma_0[1 - \Sigma\, \delta_l \cos(2\phi)$$
$$+\Lambda\cos(\alpha)(-\delta_l \mathbf{H}\sin(2\phi) + \delta_\odot \mathbf{F})$$
$$-\Lambda\sin(\alpha)(-\mathbf{T} + \delta_l \mathbf{P}\cos(2\phi))$$
$$-\Lambda_z(-\delta_l \mathbf{G}\sin(2\phi) + \delta_\odot \mathbf{E})]$$

$\delta_\odot(\delta_l)$: degree of beam pol.

Λ : degree of target pol.

First Measurements of F, H, P in $\vec{\gamma}\vec{p} \to p\omega$

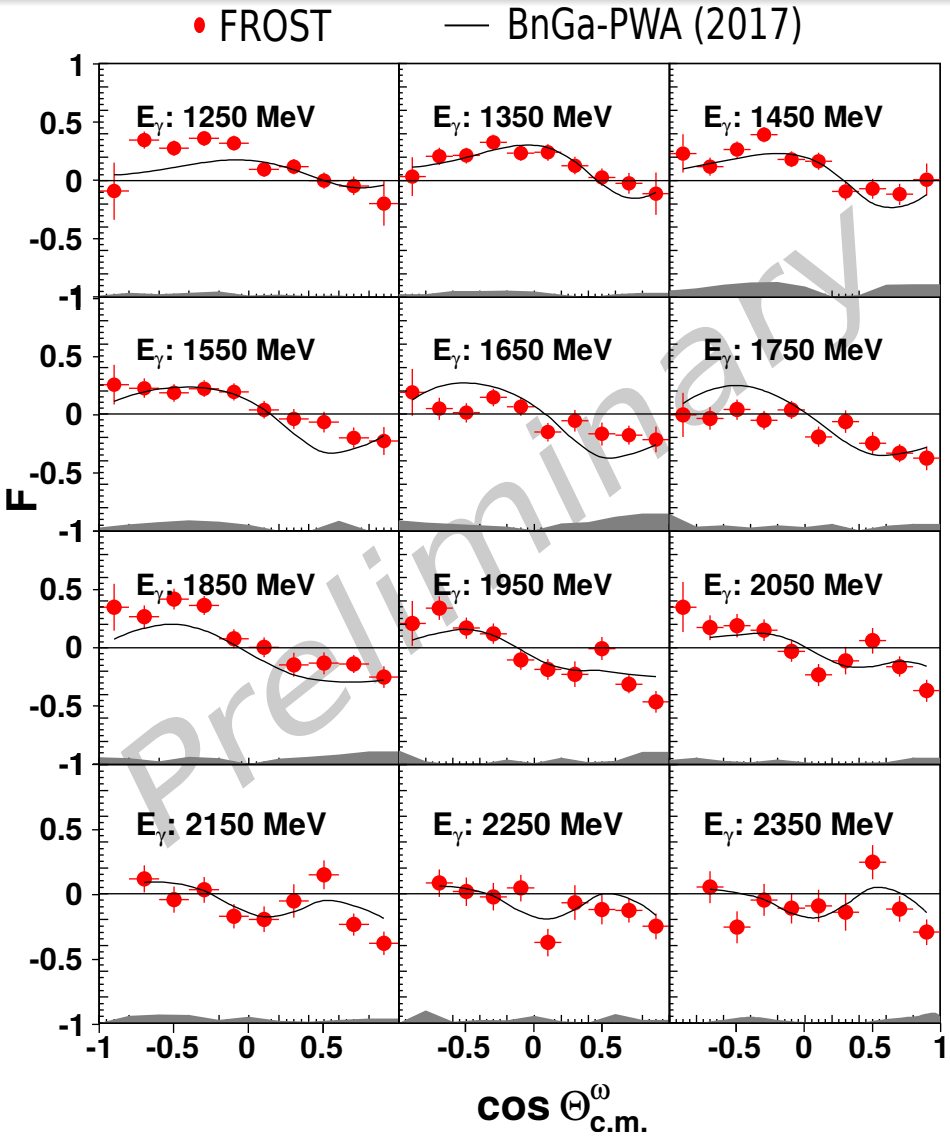

P. Roy *et al.* (CLAS-FROST), paper under preparation

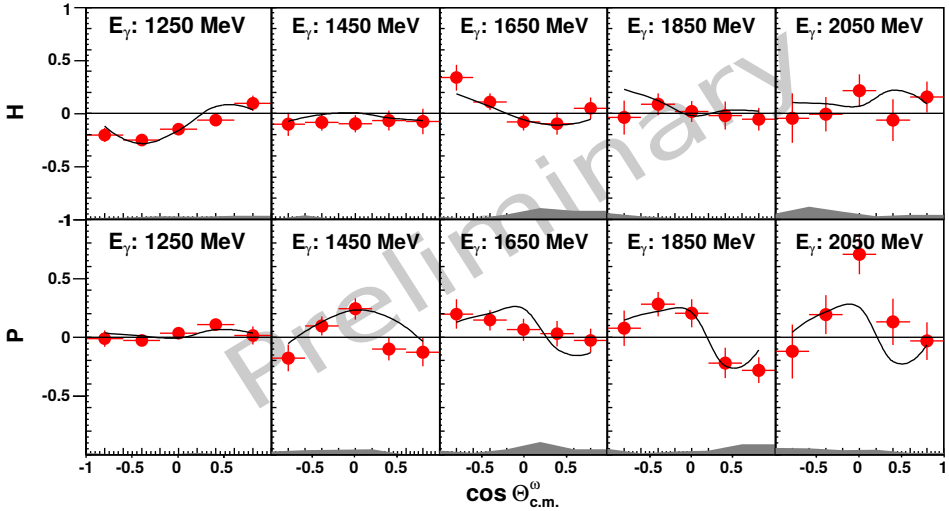

$$\sigma = \sigma_0[1 - \mathbf{\Sigma}\,\delta_l\cos(2\phi)$$
$$+\Lambda\cos(\alpha)(-\delta_l\mathbf{H}\sin(2\phi) + \delta_\odot\mathbf{F})$$
$$-\Lambda\sin(\alpha)(-\mathbf{T} + \delta_l\mathbf{P}\cos(2\phi))$$
$$-\Lambda_z(-\delta_l\mathbf{G}\sin(2\phi) + \delta_\odot\mathbf{E})]$$

$\delta_\odot(\delta_l)$: degree of beam pol.
Λ : degree of target pol.

Partial Wave Analysis of $\gamma p \to p\omega$ Observables

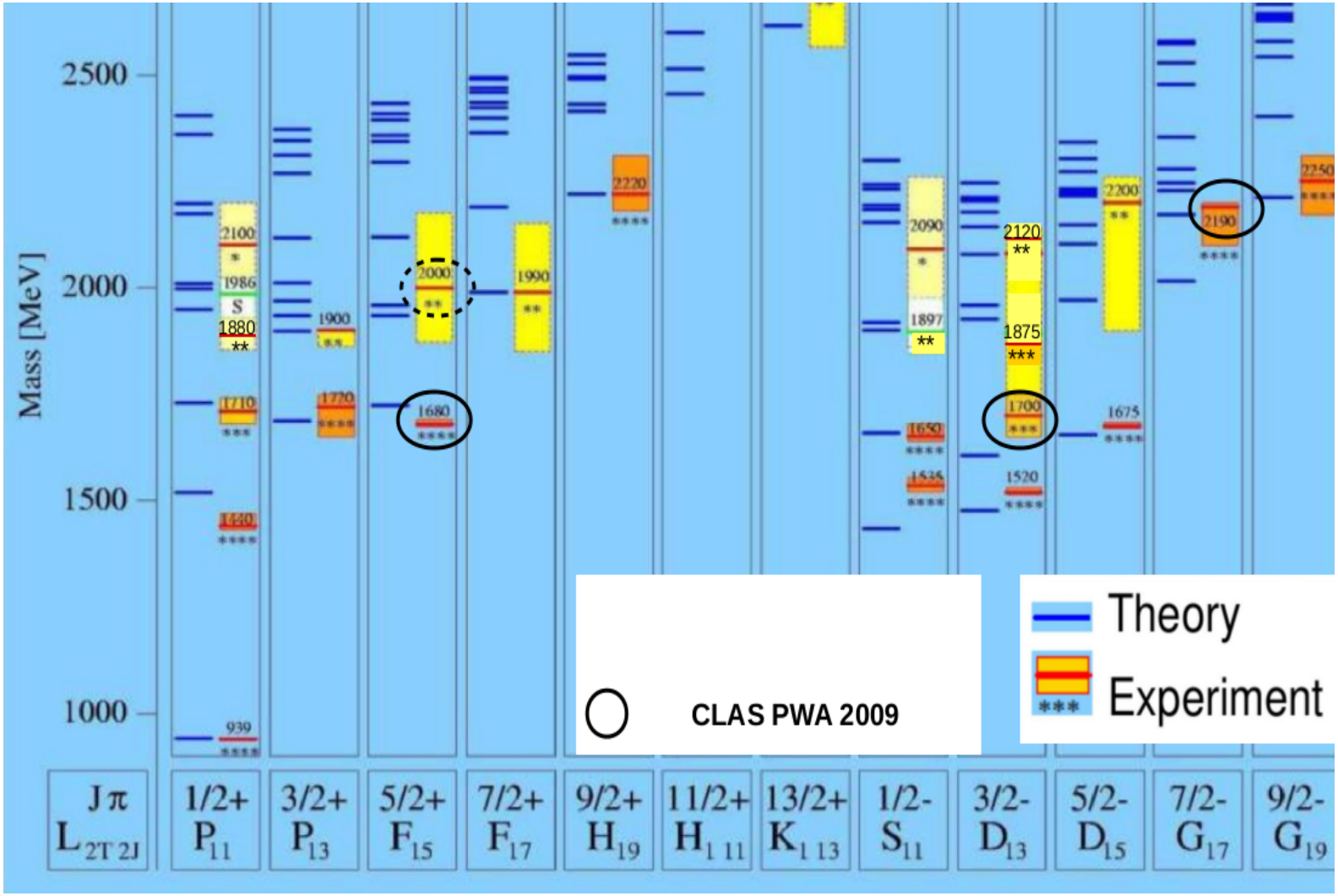

Williams *et al.*, PRC **80**, 065208 (2009)

Partial Wave Analysis of $\gamma p \to p\omega$ Observables

Polarized measurements crucial to understand the *t*-channel background

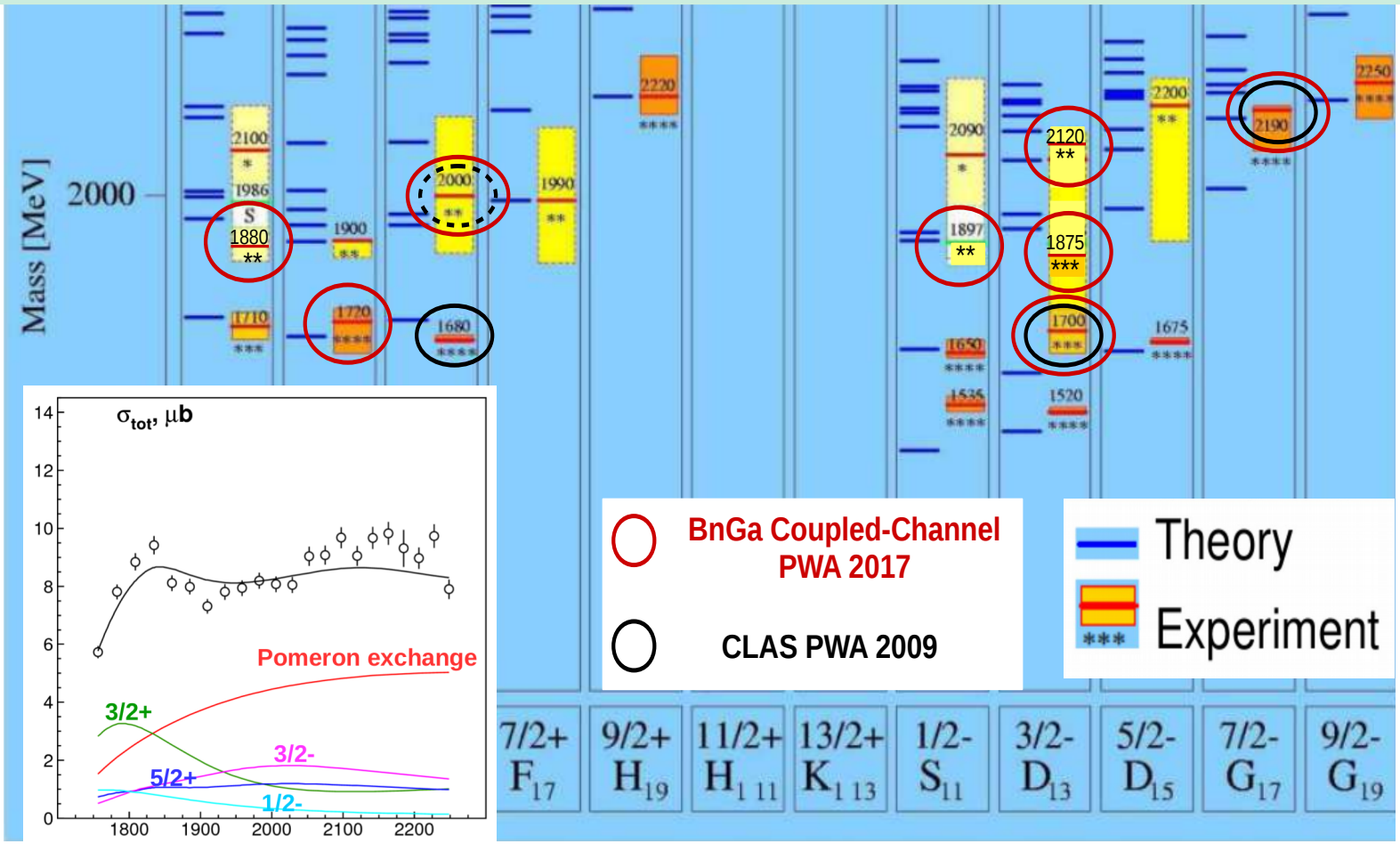

Williams *et al.*, PRC **80** (2009)
Denisenko *et al.*, Phys. Lett. B **755** (2016)

Partial Wave Analysis of $\gamma p \to p\omega$ Observables

$3/2^+$ remains leading resonant partial wave close to threshold with strong peak @ N(1720)$3/2^+$

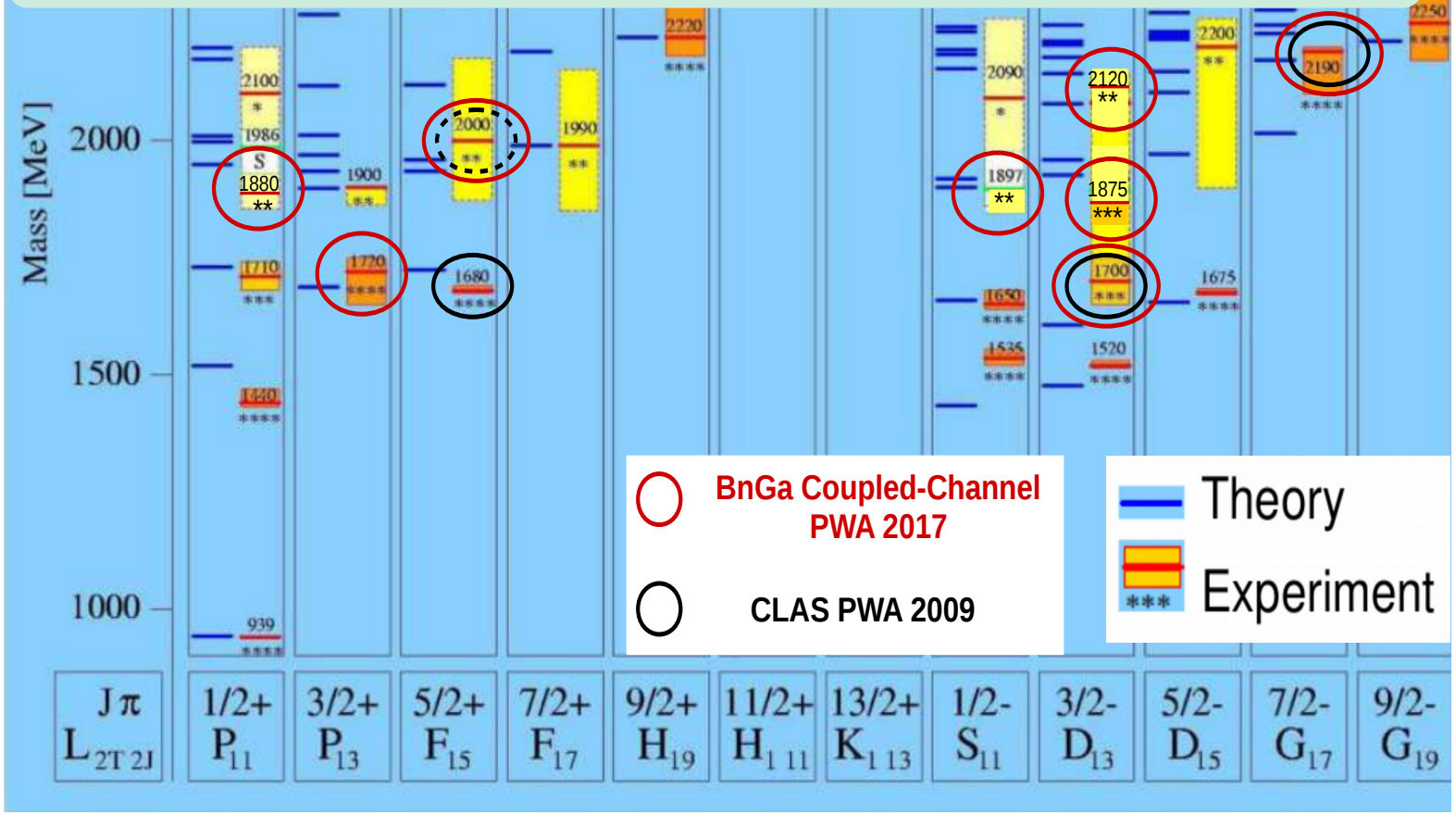

Partial Wave Analysis of $\gamma p \to p\omega$ Observables

$N\omega$ coupling of poorly-established N(2000)5/2$^+$ has increased by 1.5 times compared to previous BnGa ω-PWA

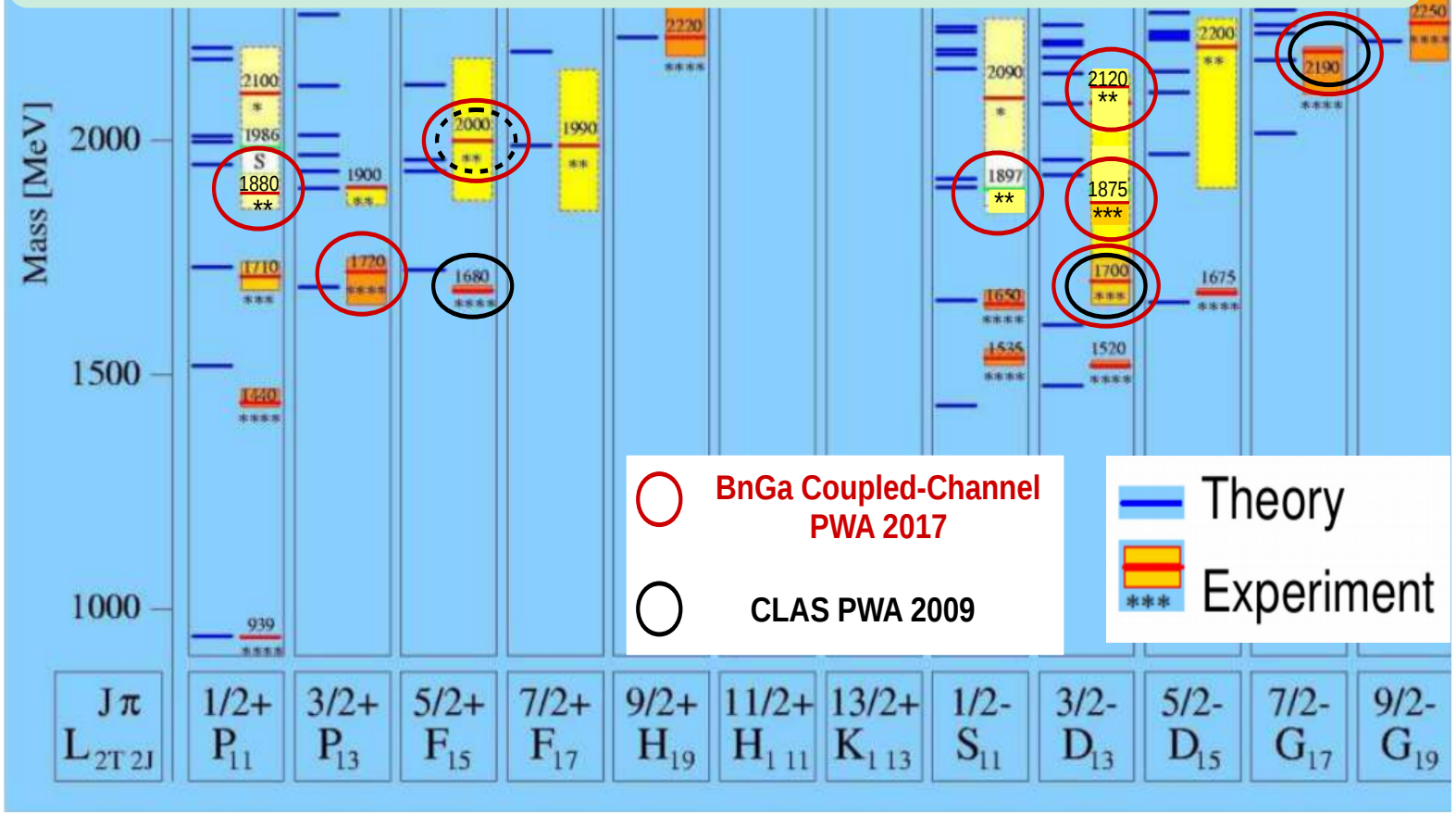

Partial Wave Analysis of $\gamma p \to p\omega$ Observables

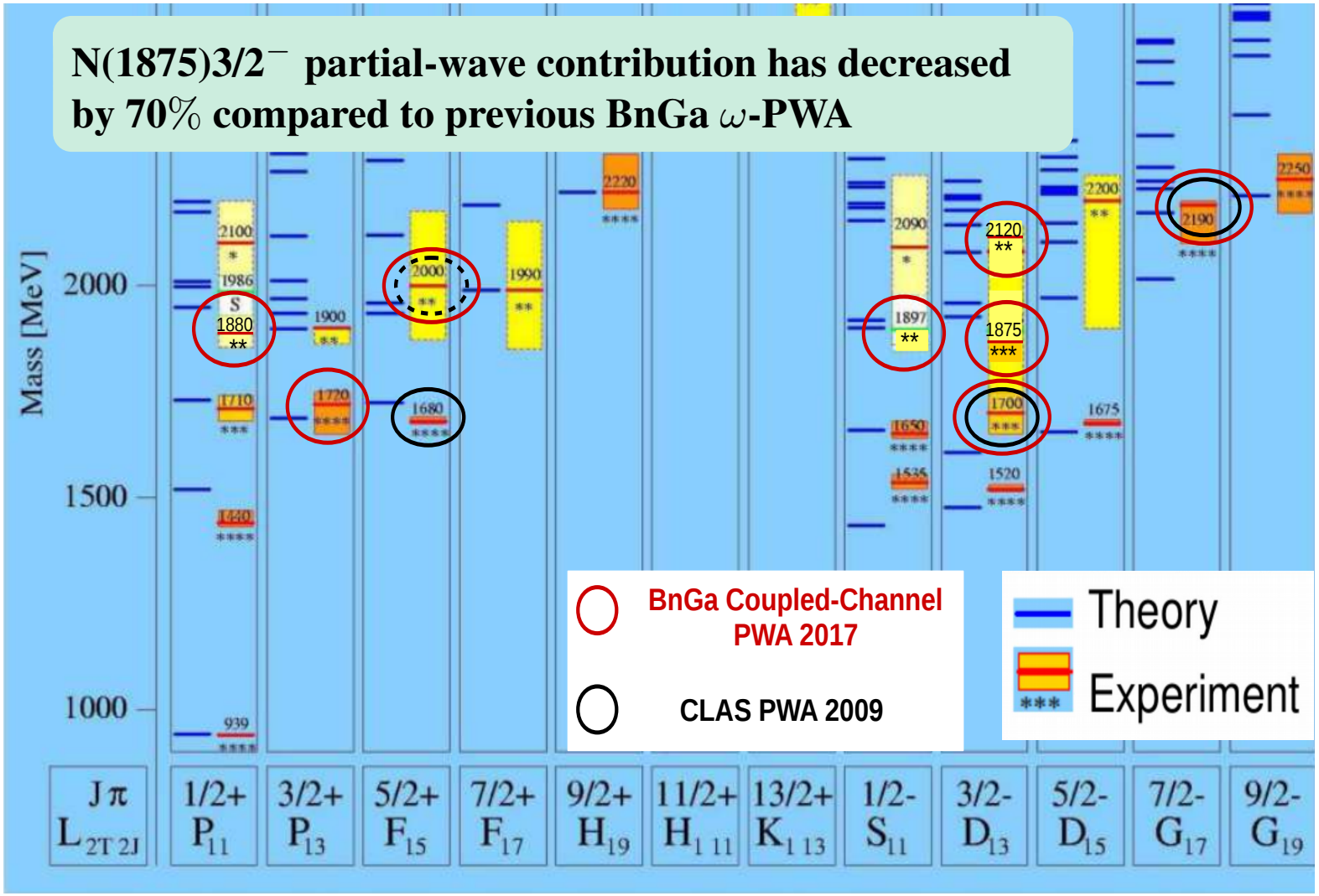

Partial Wave Analysis of $\gamma p \to p\omega$ Observables

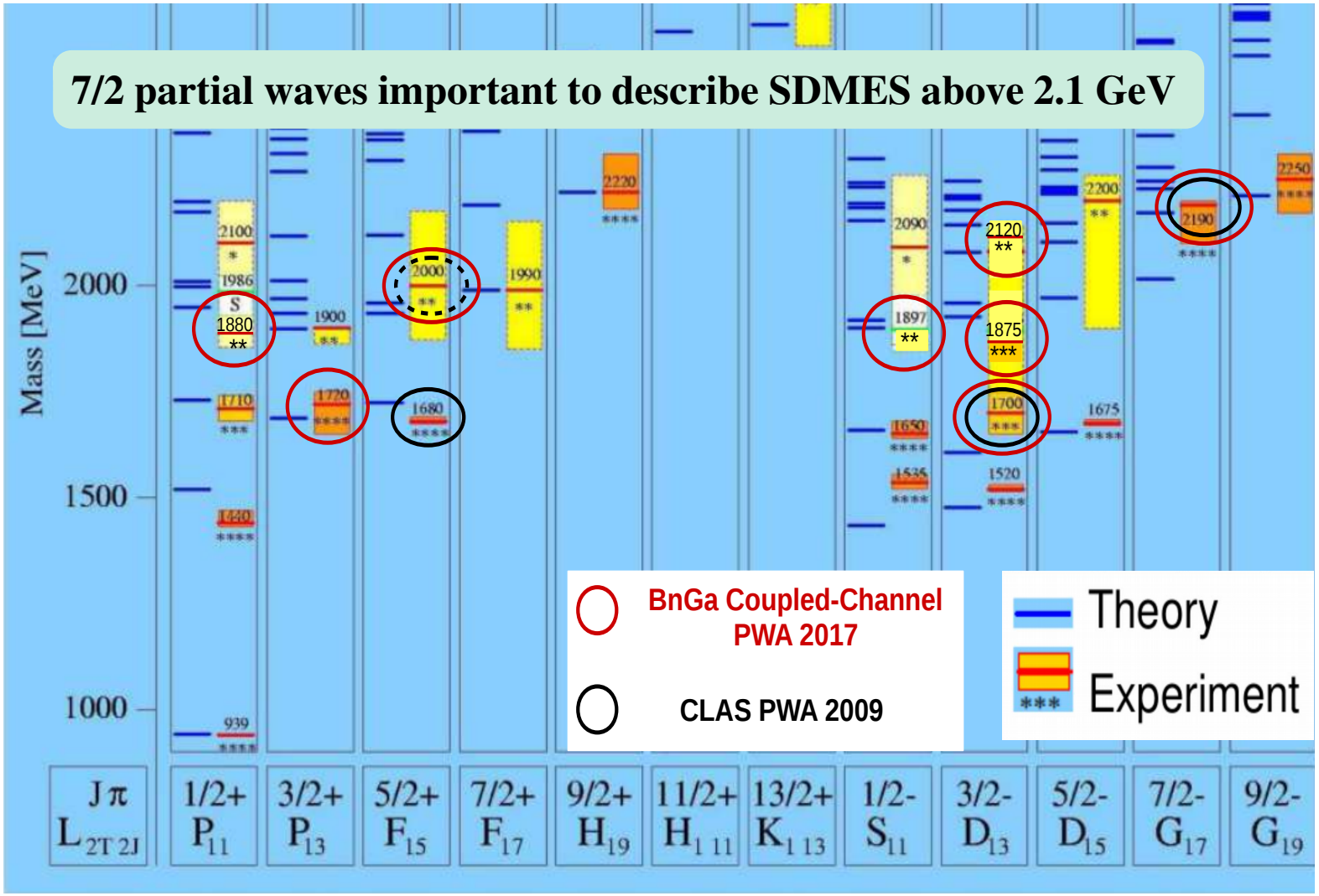

Results

Results in $\vec{\gamma}\vec{p} \to p\pi^+\pi^-$

Beam Asymmetry I^s in $\vec{\gamma}p \to p\pi^+\pi^-$

Example: $1.30 < E_\gamma < 1.40$ GeV (Total E_γ range covered: 0.7 - 2.1 GeV)

- FROST (preliminary)
- C. Hanretty *et al.* , CLAS-g8b run (in preparation for publication)

— Fourier sine fit to g8b

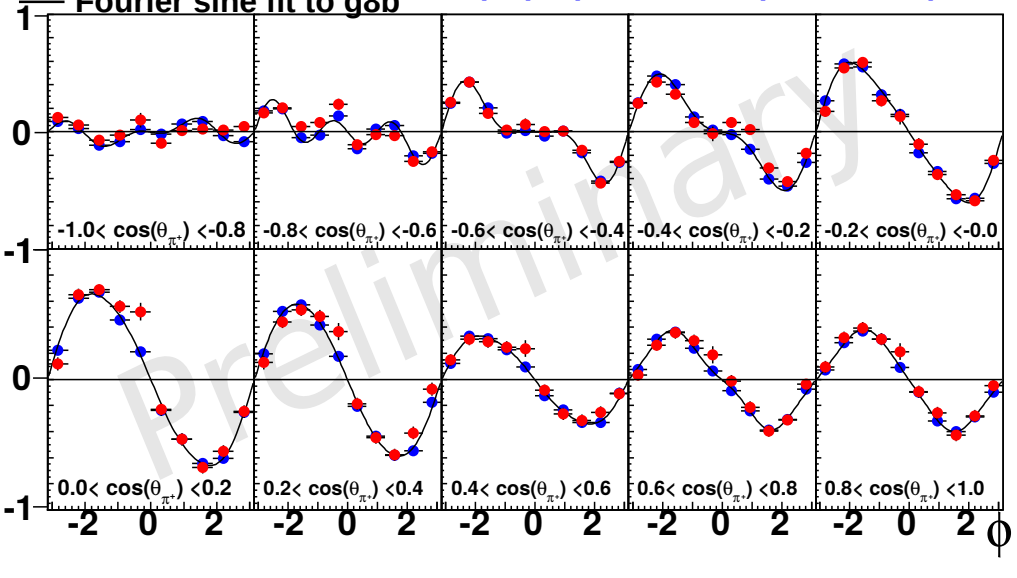

— BnGa fits to I^s, CLAS-g8b run

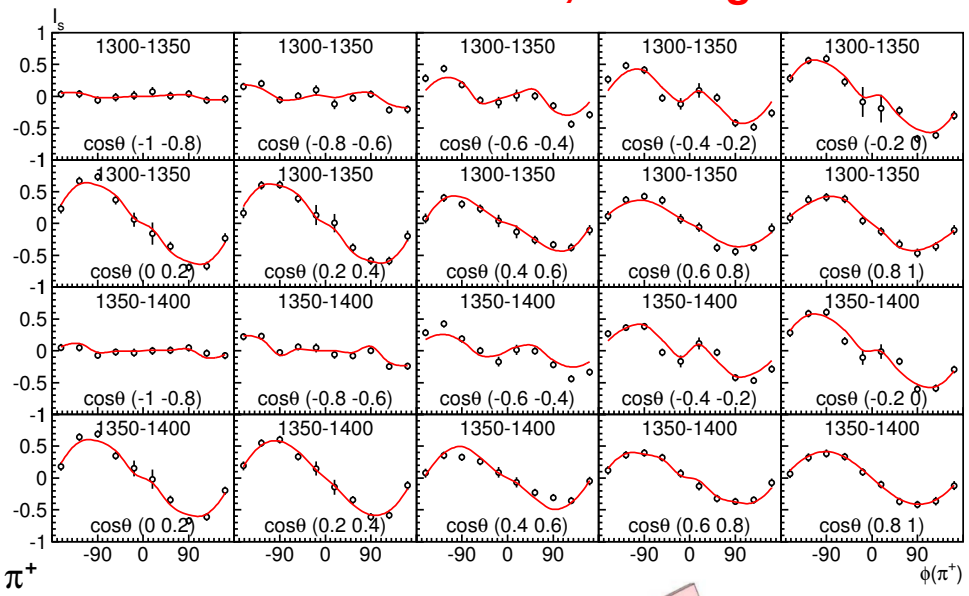

Good agreement between experiments

$$I = I_0\{\delta_l[I^s\sin(2\beta) + I^c\cos(2\beta)]\}$$

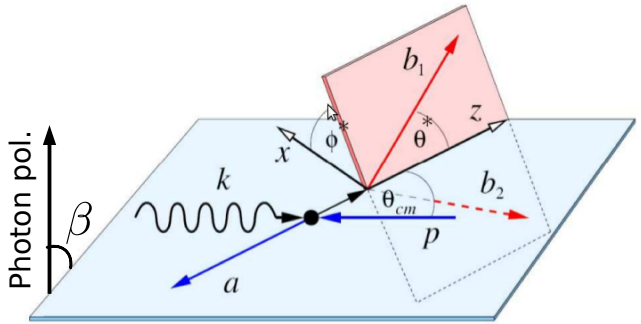

Outline

Summary

- **Photoproduction of vector mesons and multi-pion final states**: essential to **discover new resonances** and better understand the known resonances.
- **Many first-time measurements** from CLAS-FROST for $\vec{\gamma}\vec{p} \to p\omega$ (Σ (for $E_\gamma > 1.7$ GeV), T, H, P, F) and $\vec{\gamma}\vec{p} \to p\pi^+\pi^-$ ($I^{s,c}$, $P_{x,y}$, $P^{s,c}_{x,y}$): they will **significantly augment the world database** of polarization observables in photoproduction.
- **The high-quality FROST results are expected to put tight constraints on data interpretation tools**, immensely aiding in determining contributing N^* with minimal ambiguities.
- Our findings from FROST on the N^* members, together with the findings on the strange members (e.g. from PANDA at GSI, BES at Beijing, GlueX at JLab) of the multiplets will complete the study of the light baryon spectrum. This will give more insight into the phenomenon of color confinement in the system of light quarks.

Next Quest: Proton Radius Puzzle & MUSE

- Post doctoral fellow at Univ. Michigan cryotarget group which is responsible for the design, fabrication & installation of the LH_2 cryotarget assembly for MUSE.

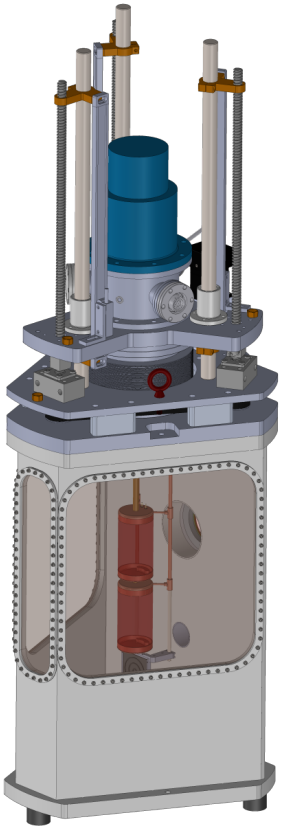

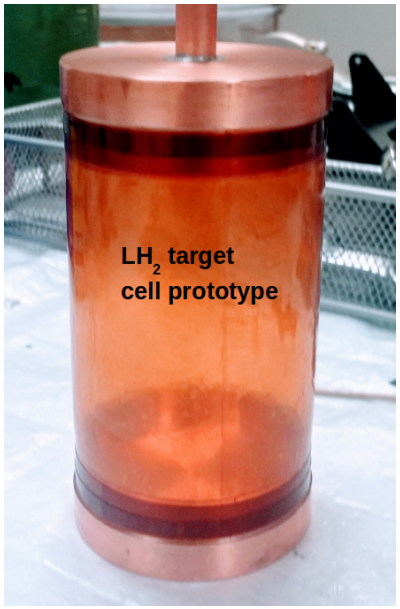

University of Michigan

Next Quest: Proton Radius Puzzle & MUSE @ PSI

- Post doctoral fellow at Univ. Michigan cryotarget group which is responsible for the design, fabrication & installation of the LH_2 cryotarget assembly for MUSE.
- The proton electric radius puzzle: discrepancy between electronic and muonic measurements to $> 7\sigma$. Novel physics or two-photon exchange effects?
- **MUSE**: first experiment to simultaneously perform μ and e elastic measurements and compare results with reduced systematics. Discrepancies, if real, will be confirmed with $5\,\sigma$ significance.
  Q^2 **coverage**: $0.00016 - 0.08$ GeV^2.

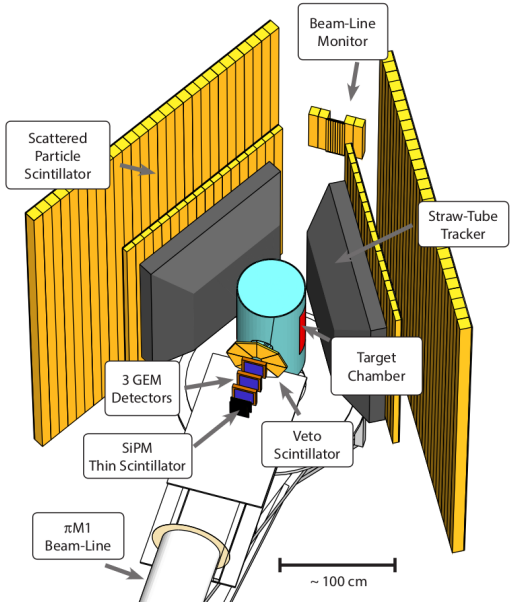

Next Quest: Proton Radius Puzzle & MUSE @ PSI

- Post doctoral fellow at Univ. Michigan cryotarget group which is responsible for the design, fabrication & installation of the LH_2 cryotarget assembly for MUSE.
- The proton electric radius puzzle: discrepancy between electronic and muonic measurements to $> 7\sigma$. Novel physics or two-photon exchange effects?
- **MUSE**: first experiment to simultaneously perform μ and e elastic measurements and compare results with reduced systematics. Discrepancies, if real, will be confirmed with $5\,\sigma$ significance.
  Q^2 **coverage**: $0.00016 - 0.08$ GeV^2.
- $\mu^{\pm}$ and $e^{\pm}$ measurements will allow test of $2\,\gamma$ exchange effect at sub-percent level.

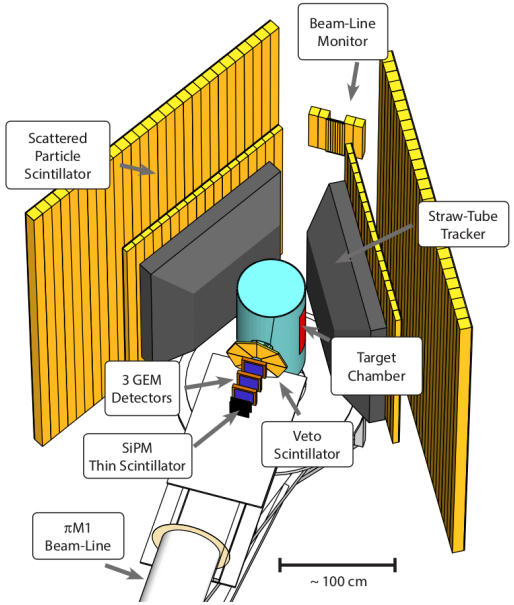

Next Quest: Proton Radius Puzzle & MUSE @ PSI

- Post doctoral fellow at Univ. Michigan cryotarget group which is responsible for the design, fabrication & installation of the LH_2 cryotarget assembly for MUSE.
- The proton electric radius puzzle: discrepancy between electronic and muonic measurements to $> 7\sigma$. Novel physics or two-photon exchange effects?
- **MUSE**: first experiment to simultaneously perform μ and e elastic measurements and compare results with reduced systematics. Discrepancies, if real, will be confirmed with $5\,\sigma$ significance.
  Q^2 **coverage**: $0.00016 - 0.08$ GeV^2.
- $\mu^{\pm}$ and $e^{\pm}$ measurements will allow test of $2\,\gamma$ exchange effect at sub-percent level.
- MUSE has 8 participating institutions. Experiment is planned to be conducted at PSI, Switzerland in Fall 2018 and 2019.

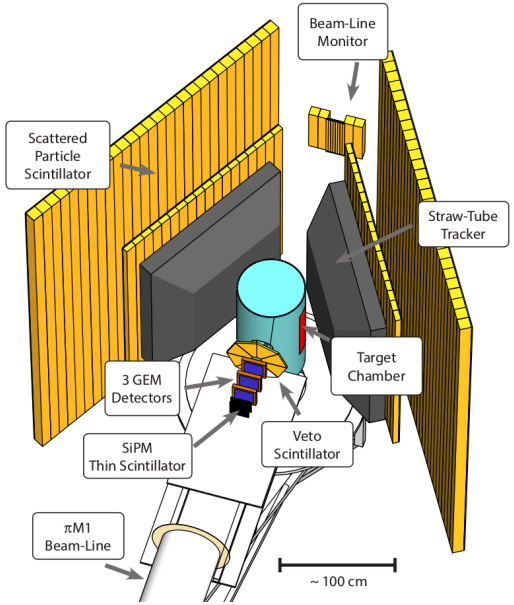

Thank You !

Acknowledgement: this thesis work was supported by U.S. DOE, Office of Science, Office of Nuclear Physics, under contract No. DE-AC05-06OR23177

Backup slides

BnGa Fits and Partial Wave Contributions

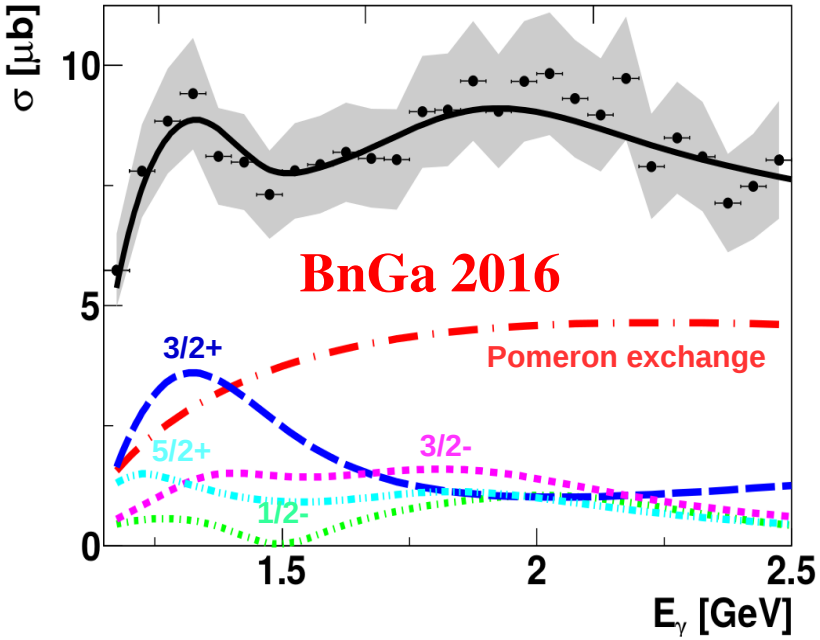

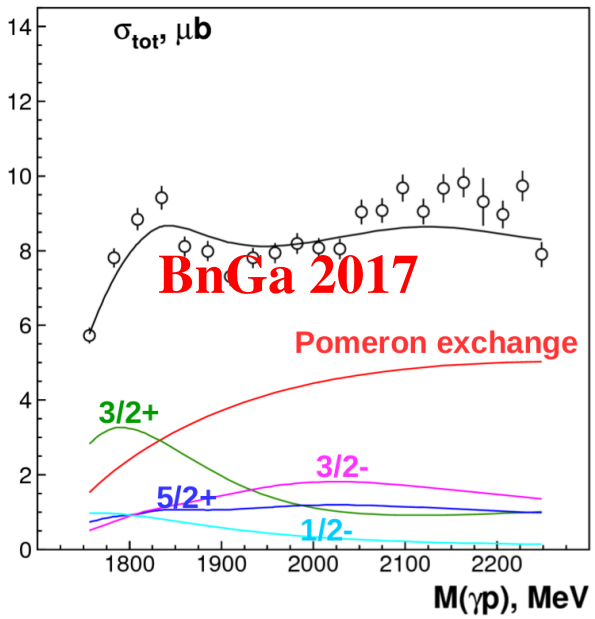

- N(1875)3/2$^-$ contribution decreased by 70%.
- N(2100)3/2$^-$ contribution did not change notably, but phase changed leading to smoother structure.
- N(1895)1/2$^-$ coupling changed very little. But this partial wave has less structure because of a change in the sign of a non-resonant contribution.
- Coupling to N(2000)5/2$^+$ increased by 1.5 times.

CLAS Experiment Details

Capability	Quantity	Range
Coverage	Charged-particle angle	$8^\circ \leqslant \theta \leqslant 140^\circ$
	Charged-particle momentum	$p \geqslant 0.2$ GeV/c
	Photon angle (4 sectors)	$8^\circ \leqslant \theta \leqslant 45^\circ$
	Photon angle (2 sectors)	$8^\circ \leqslant \theta \leqslant 75^\circ$
	Photon energy	$E_\gamma \geqslant 0.1$ GeV
Resolution	Momentum ($\theta \lesssim 30^\circ$)	$\sigma_p/p \approx 0.5\%$
	Momentum ($\theta \gtrsim 30^\circ$)	$\sigma_p/p \approx$ (1–2)%
	Polar angle	$\sigma_\theta \approx 1$ mrad
	Azimuthal angle	$\sigma_\phi \approx 4$ mrad
	Time (charged particles)	$\sigma_t \approx$ (100–250) ps
	Photon energy	$\sigma_E/E \approx 10\%/\sqrt{E}$
Particle ID	π/K separation	$p \leqslant 2$ GeV/c
	π/p separation	$p \leqslant 3.5$ GeV/c
	π^- misidentified as e^-	$\leqslant 10^{-3}$
Luminosity	Electron beam	$L \approx 10^{34}$ nucleon cm^{-2} s^{-1}
	Photon beam	$L \approx 5 \times 10^{31}$ nucleon cm^{-2} s^{-1}
Data acquisition	Event rate	4 kHz
	Data rate	25 MB/s
Polarized target	Magnetic field	$B_{max} = 5$ T

Systematic Errors

Source	Systematic Uncertainty
Background subtraction	given as gray band for each distribution
Beam-polarization	5 %
Target-polarization	2 %
Target-offset angle	2 %
Normalization	
beam asymmetry	5 %
target asymmetry	2 %
Beam asymmetry	
σ_{total} (fractional only)	$\sim 7.5\,\%$
Target asymmetry	
σ_{total} (fractional only)	$\sim 3.5\,\%$

CLAS Experiment Details Continued

(1) Electron beam current: $5 - 14$ nA
(2) Electron beam energy: 3.082 GeV (circ. + lin.), 5.078 GeV (circ.)
(3) Gold foil of 10^{-4} radiation length thickness used for
creating circularly-polarized photons from longitudinally-polarized electrons.
Longitudinally-polarized electrons created by circularly-polarizing the laser
using 2 Pockel cells prior to irradiating the GaAs photocathode.
(4) Diamond radiator of thickness 50μm to produce lin. pol. photons.
The divergence of the e^- beam in the crystal increases with thickness.
More divergence leads to broader coherent peaks and a lower degree of polarization.

(1) E-T plane resolution: 110 ps
(2) Photon tagging resolution: $\Delta(E)/E = 0.1\%$
(3) Start counter resolution: 290 ps at the straight section, 320 ps at the nose
(4) TOF resolution: 80 ps for short counters, 160 ps for the long counters
(5) Average time resolution for reconstructed electrons in CLAS: 150 ps

The Horizontal Dilution Refrigerator

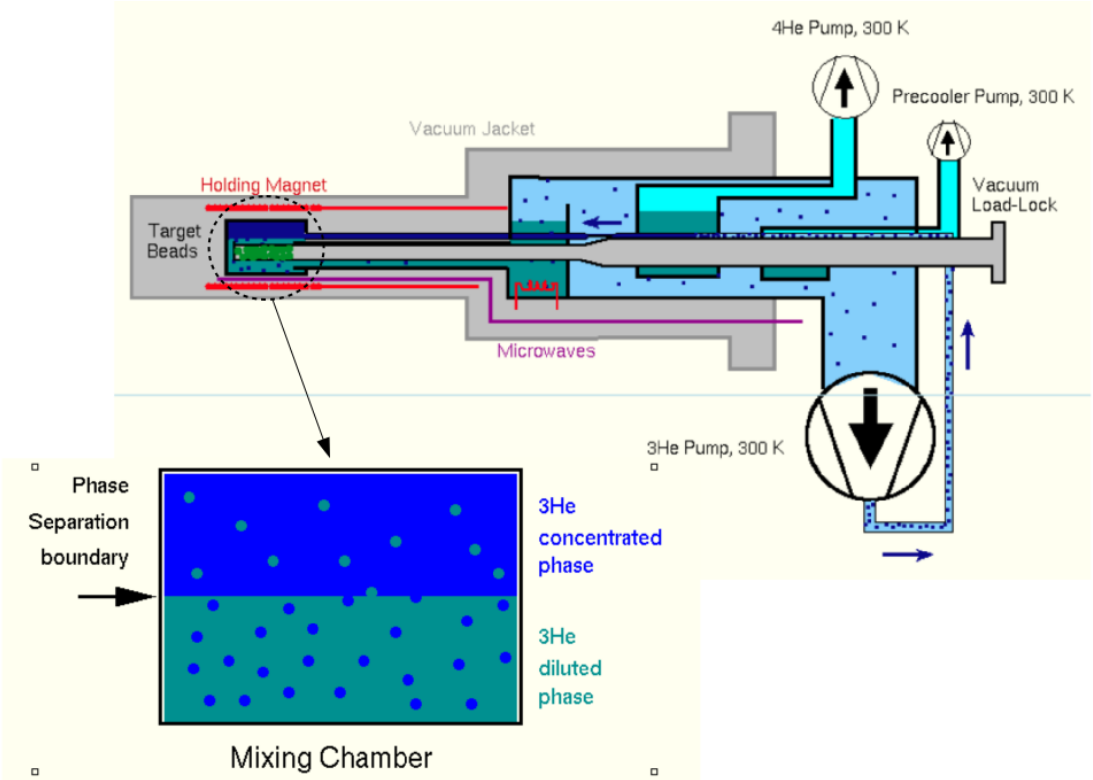

Below 0.8 K, the ^{3}He-^{4}He mixture separated into two phases:
^{3}He rich (specific heat = 22 J/(mol K)),
^{3}He poor (specific heat = 106 J(mol K)).

Due to the difference in the specific heat, ^{3}He absorbs heat from its surrounding while traveling from the concentrated phase to the dilute phase.

Photoproduction Cross Section

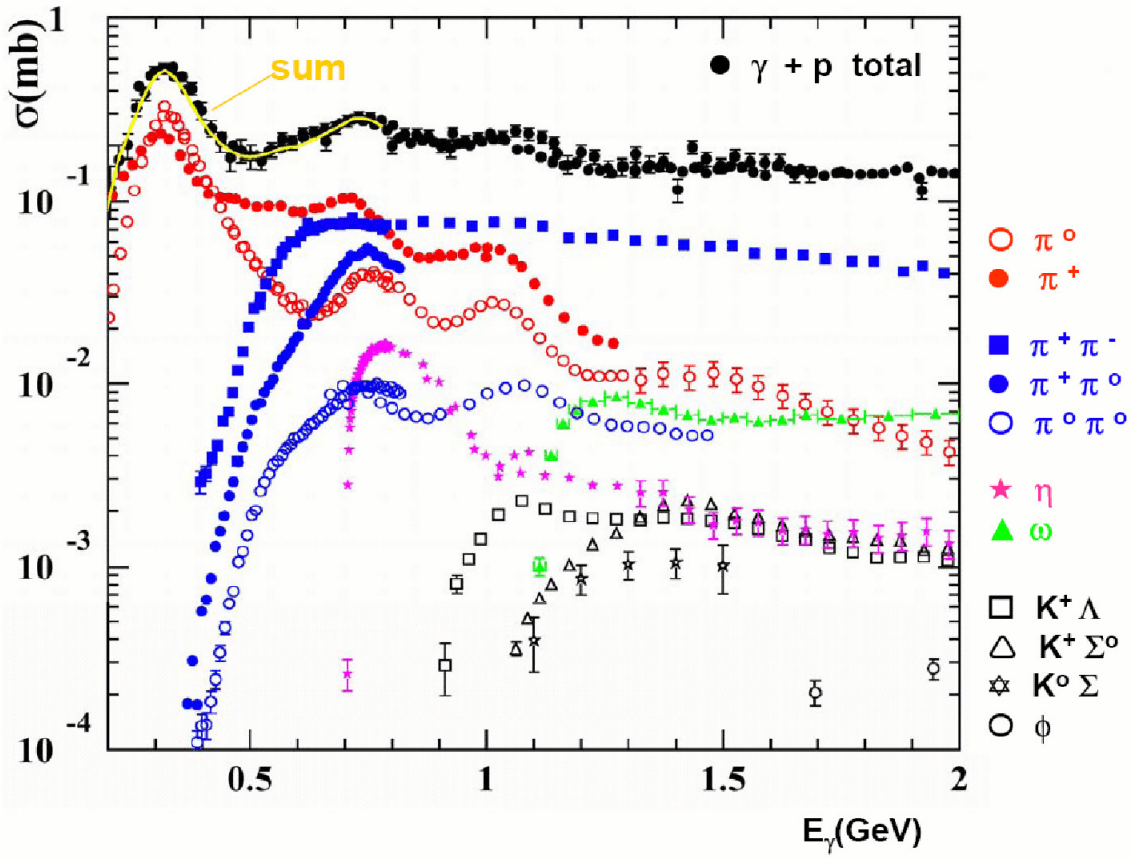

Photon Selection Cuts

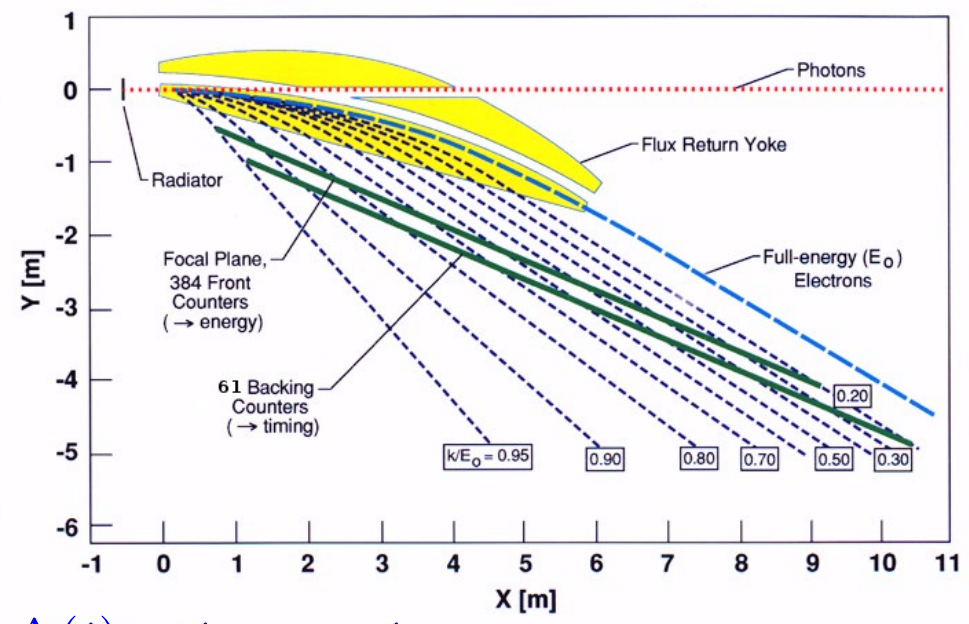

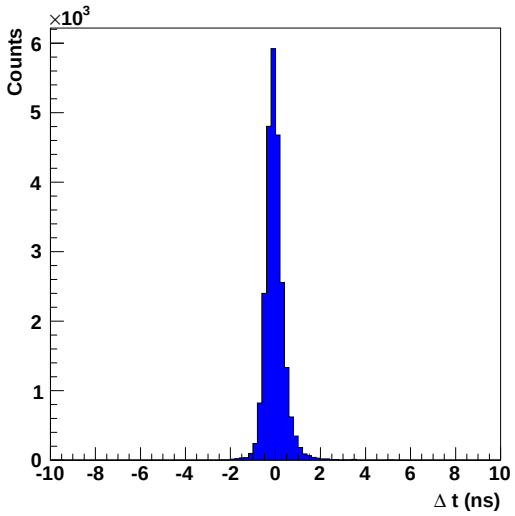

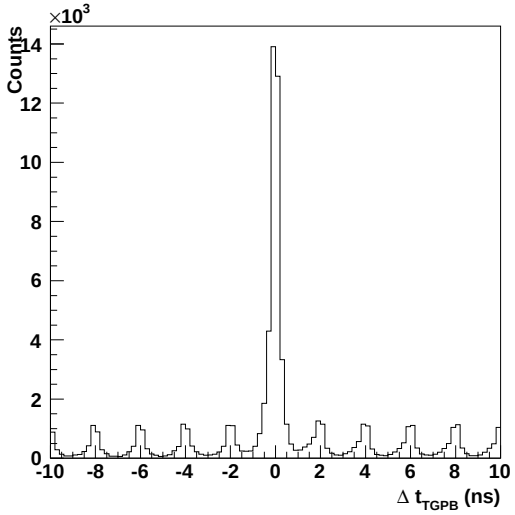

$\Delta(t) = t_{\text{event}} - t_{\gamma}$

~ 5 candidate photons per event on average.

Cuts applied:

1) $|\Delta(t)| < 1$ ns

2) Only 1 candidate photon in the same RF bucket and all tracks of the event originate from the same tagged photon ($88 - 90\%$ events).

β cut

$$\beta_{cal} = \frac{p_{DC}}{\sqrt{{p_{DC}}^2 + m^2}}$$

$$\beta_{meas} = \frac{v_{TOF}}{c}$$

$$\Delta\beta = \beta_{cal} - \beta_{meas}$$

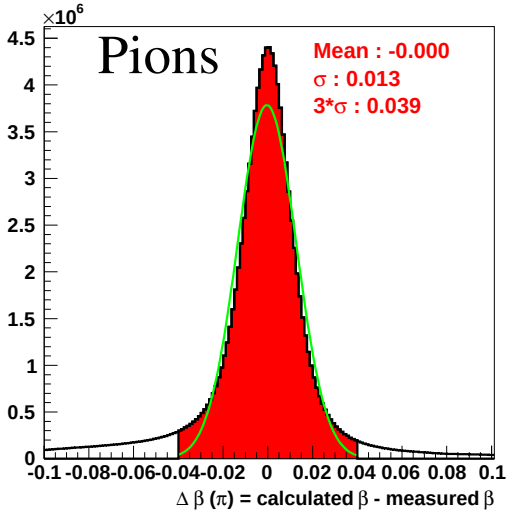

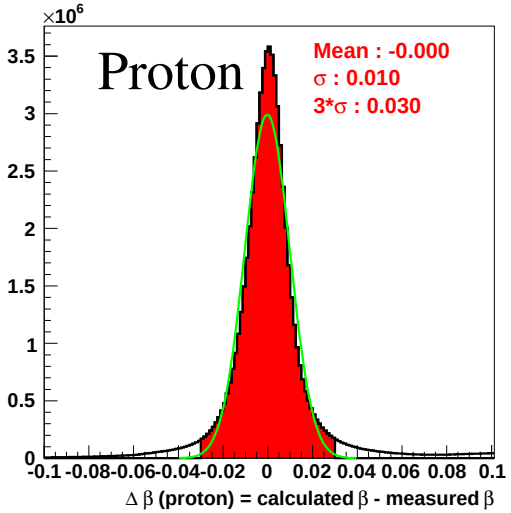

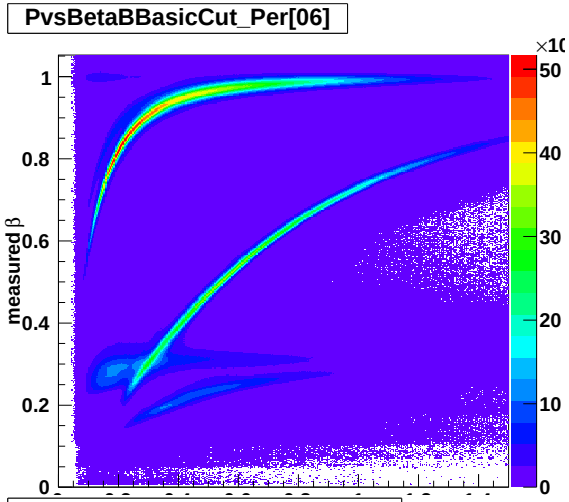

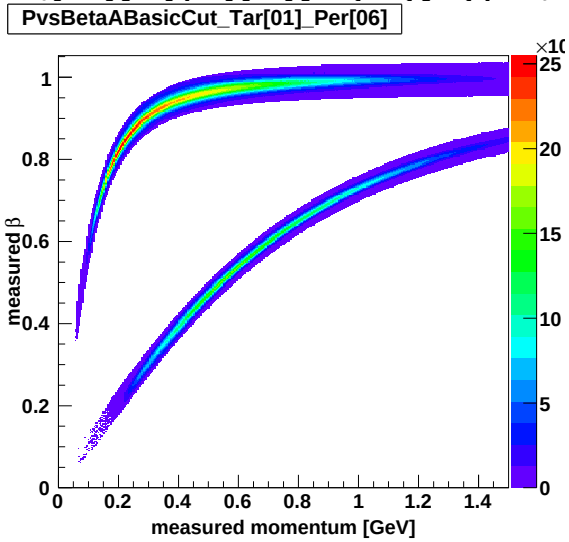

Event Statistics after Various Cuts

Cuts	# of Events (% of Events)			
No cut	1.031e09 (100)			
Vertex Cut (Butanol Events)	6.74e07 (6.5)			
Vertex Cut + Topology Cut	Topology 1	Topology 2	Topology 3	Topology 4
	2.05e07 (1.99)	1.99e07 (1.93)	1.71e07 (1.66)	1.00e07 (0.97)
Vertex Cut + Topology Cut + Photon Selection Cuts	1.16e07 (1.13)	9.83e06 (0.95)	1.12e07 (1.09)	6.30e06 (0.61)
Vertex Cut + Topology Cut + Photon Selection + β Cut	8.43e06 (0.82)	7.72e06 (0.75)	6.54e06 (0.63)	4.01e06 (0.39)

Event-Based Qfactor Method with Likelihood Fits

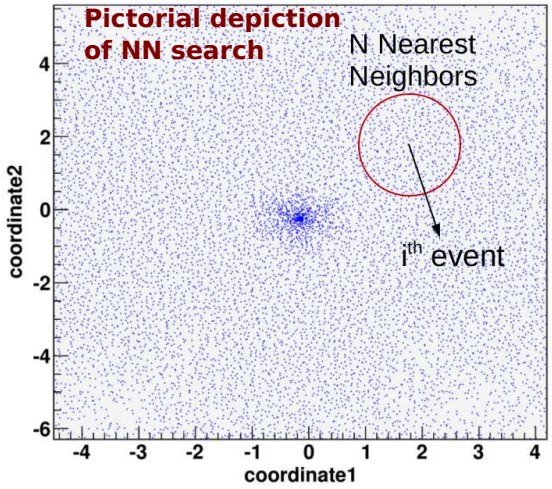

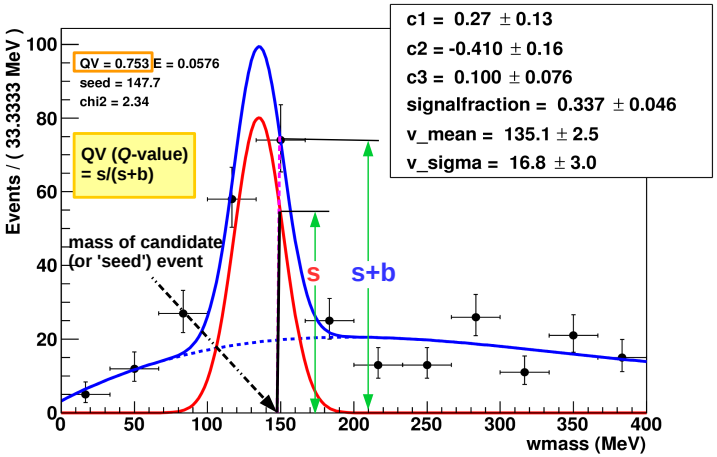

- **A multivariate analysis -** For each event ("seed event"), find N nearest neighbors in $N-$D kinematic phase space (e.g. λ, θ_{HEL}, ϕ_{HEL}, $\cos(\theta^p)_{c.m.}$, $\phi^{p_{\rm recoil}}_{\rm c.m.}$ for ω analysis). Plot mass distribution of the $N+1$ events and fit.
- Since N is small (300), use ML method to fit the mass distribution.
  $L = \prod_i [f^{Signal}(m_i, \alpha) + f^{Bkg}(m_i, \beta)]$

  $\mathbf{Q_{seed-event}} = \frac{f^{Signal}(m_0, \alpha^{best})}{[f^{Signal}(m_0, \alpha^{best}) + f^{Bkg}(m_0, \beta^{best})]}$, m_0- seed event's mass.

Fenyman Diagrams for 2-pion Photoproduction

Image Source: J. Ahrens *et al.*, EPJ A **34**, 11 (2007).

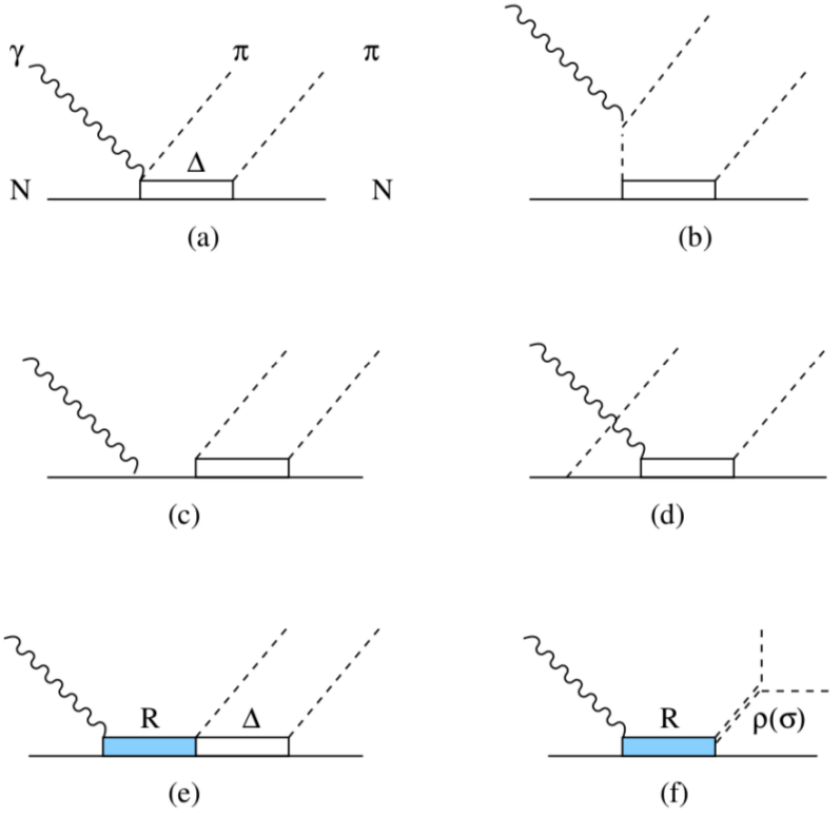

Figure 1.12: Feynman diagrams for two-pion photoproduction. a) Δ-Kroll-Ruderman term, b) Δ pion-pole term, c) Δ exchange term, d) direct Born term, e)-f) resonance terms.

Published Results in $\vec{\gamma}\vec{p} \to p\pi^+\pi^-$

- Allow the study of sequential decays of intermediate N^* and also $N^* \to p\rho$ decay but the large hadronic background makes it challenging.
- Reaction described using 2 planes (5 kinematic variables) $\to$ more spin observables than in single-meson photoproduction using polarized beam and target.

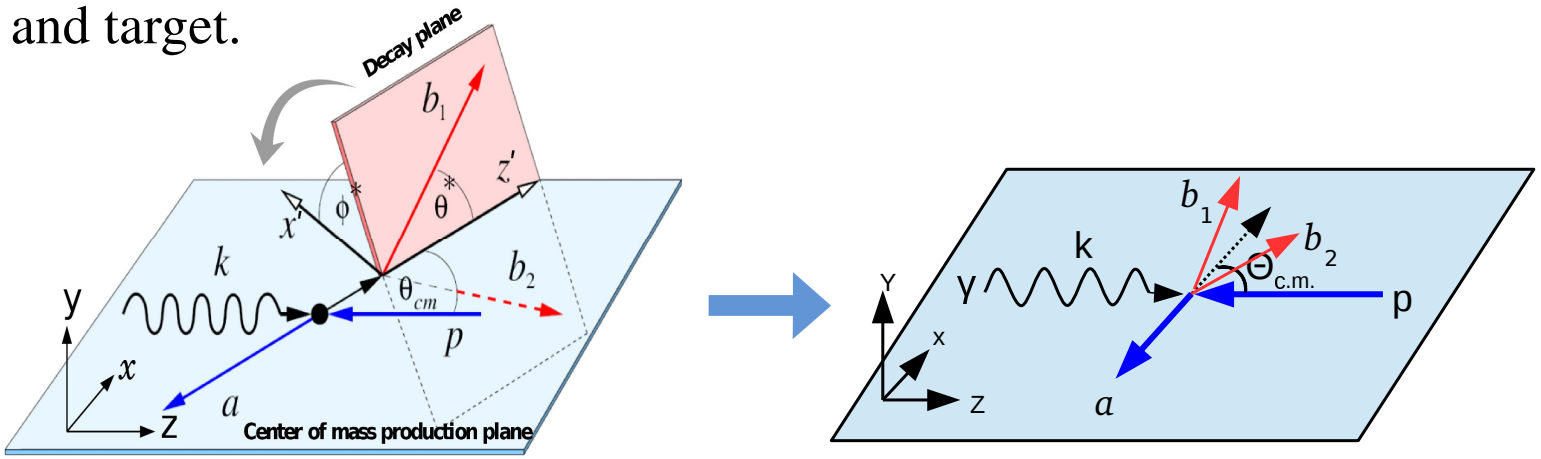

2 beam-pol. observables: I^s, I^c
Unlike only one (Σ observable) in single-meson photoproduction.

I^s vanishes, I^c survives.

W. Roberts and T. Oed, PRC **71**, 055201 (2005)

Why are Spin Observables Important?

[1] R. Bradford *et al.* (CLAS), PRC **75**, 035205 (2007), Observables C_x, C_z from $\vec{\gamma}p \rightarrow K^+\vec{\Lambda}$
[2] Fits: BnGa Model, V.A. Nikonov *et al.*, Phy. Lett. B **662**, 245 (2008)

C_x, C_z Fits without N(1900)3/2$^+$ resonance

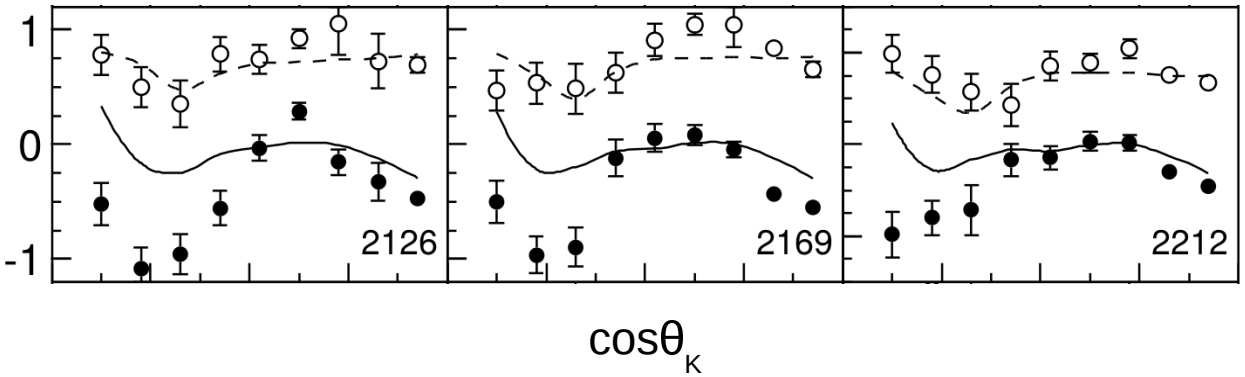

C_x, C_z Better Fit Results with N(1900)3/2$^+$!

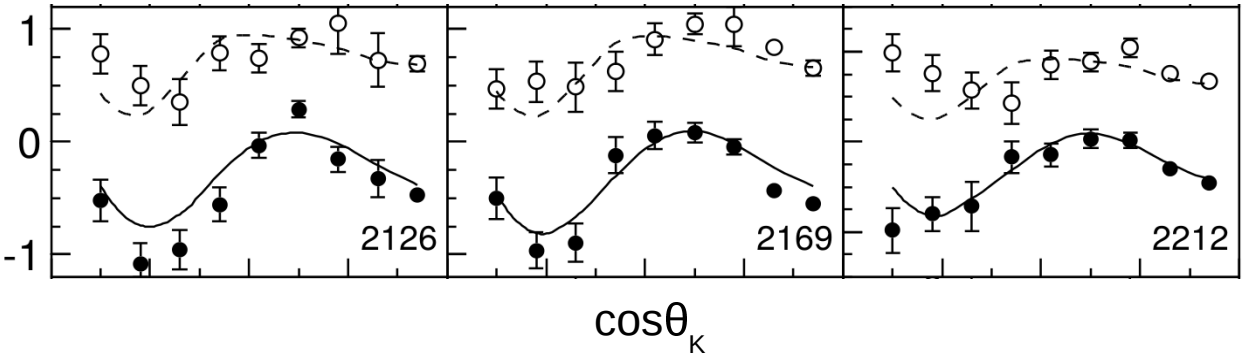

Currently 17 N^* and 10 Δ^* with at least (∗∗∗) rating.

N^*	J^P $(L_{2I,2J})$	2010	2012
$N(1440)$	$1/2^+$ (P_{11})	∗∗∗∗	∗∗∗∗
$N(1520)$	$3/2^-$ (D_{13})	∗∗∗∗	∗∗∗∗
$N(1535)$	$1/2^-$ (S_{11})	∗∗∗∗	∗∗∗∗
$N(1650)$	$1/2^-$ (S_{11})	∗∗∗∗	∗∗∗∗
$N(1675)$	$5/2^-$ (D_{15})	∗∗∗∗	∗∗∗∗
$N(1680)$	$5/2^+$ (F_{15})	∗∗∗∗	∗∗∗∗
$N(1685)$			∗
$N(1700)$	$3/2^-$ (D_{13})	∗∗∗	∗∗∗
$N(1710)$	$1/2^+$ (P_{11})	∗∗∗	∗∗∗
$N(1720)$	$3/2^+$ (P_{13})	∗∗∗∗	∗∗∗∗
$N(1860)$	$5/2^+$		∗∗
$N(1875)$	$3/2^-$		∗∗∗
$N(1880)$	$1/2^+$		∗∗
$N(1895)$	$1/2^-$		∗∗
$N(1900)$	$3/2^+$ (P_{13})	∗∗	∗∗∗
$N(1990)$	$7/2^+$ (F_{17})	∗∗	∗∗
$N(2000)$	$5/2^+$ (F_{15})	∗∗	∗∗
~~$N(2080)$~~	D_{13}	∗∗	
~~$N(2090)$~~	S_{11}	∗	
$N(2040)$	$3/2^+$		∗
$N(2060)$	$5/2^-$		∗∗
$N(2100)$	$1/2^+$ (P_{11})	∗	∗
$N(2120)$	$3/2^-$		∗∗
$N(2190)$	$7/2^-$ (G_{17})	∗∗∗∗	∗∗∗∗
~~$N(2200)$~~	D_{15}	∗∗	
$N(2220)$	$9/2^+$ (H_{19})	∗∗∗∗	∗∗∗∗

First Measurements of Target Asymmetry T in $\gamma\vec{p} \rightarrow p\omega$

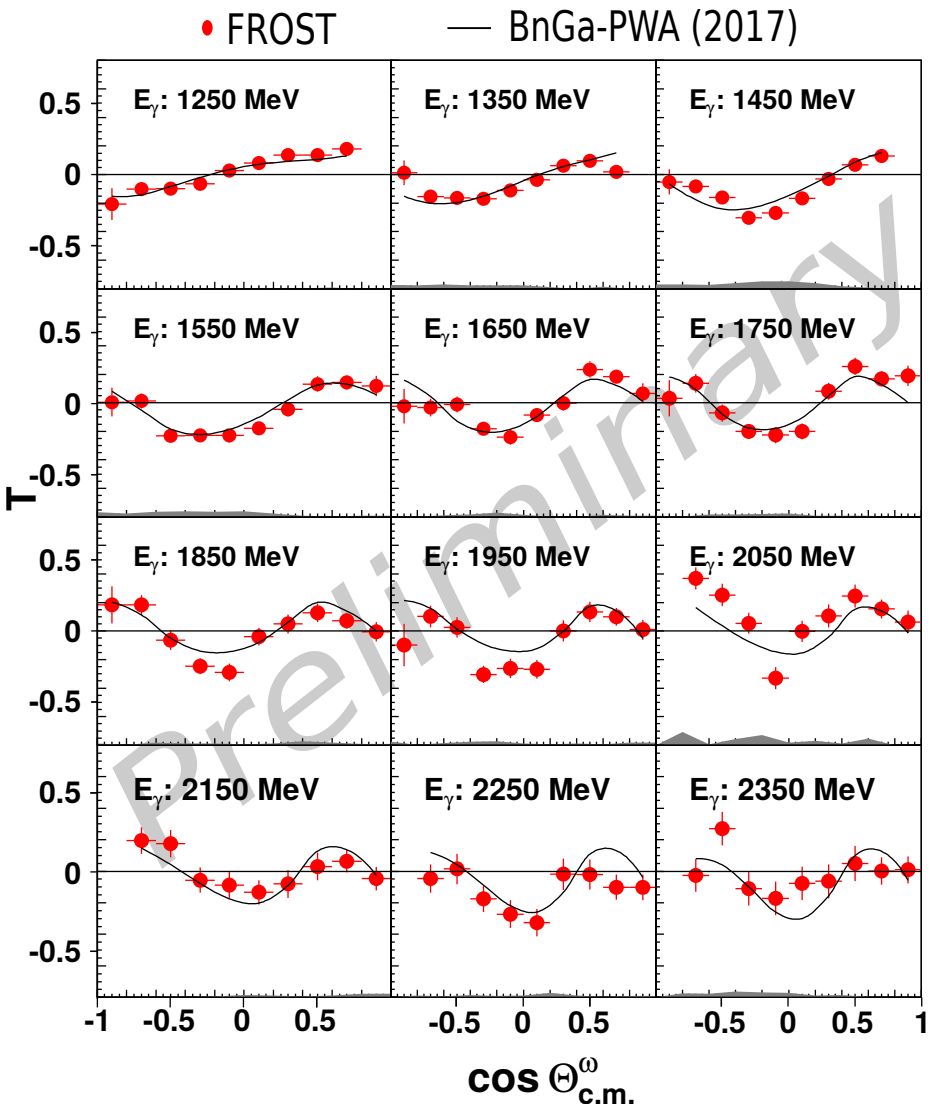

P. Roy *et al.* (CLAS-FROST), paper under review

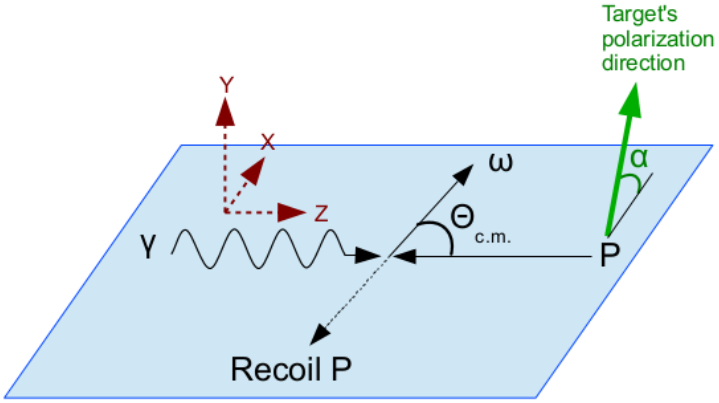

$$\sigma = \sigma_0[1 - \mathbf{\Sigma}\,\delta_l\cos(2\phi)$$
$$+\Lambda\cos(\alpha)(-\delta_l\mathbf{H}\sin(2\phi) + \delta_\odot\mathbf{F})$$
$$-\Lambda\sin(\alpha)(-\mathbf{T} + \delta_l\mathbf{P}\cos(2\phi))$$
$$-\Lambda_z(-\delta_l\mathbf{G}\sin(2\phi) + \delta_\odot\mathbf{E})]$$

$\delta_\odot(\delta_l)$: degree of beam pol.
Λ : degree of target pol.

Scattering Amplitudes in $\gamma p \to p\pi^+\pi^-$ and $\gamma p \to p\omega$

$\gamma p \to p\pi^+\pi^-$ reaction: Roberts and Oed, PRC **71**, 055201 (2015)

- 8 independent helicity amplitudes after parity invariance operation.
- Need 15 carefully selected observables at each kinematic bin for fully determining the helicity amplitudes.
- A complete measurement will require certain single, double and triple polarization observables in addition to the differential cross section.

$\gamma p \to p\omega$ reaction: Pichowsky *et al.*, PRC **53** (1996)

- 12 independent helicity amplitudes after parity invariance.
- 8 single spin, 51 double spin, 123 triple spin and 108 quadrupole spin (γ, p, $p^{'}$, vector and tensor pol. of ω) observables after parity conservation.
- Need 23 carefully selected observables for determining the helicity amplitudes.
- A complete experiment doesn't seem plausible, but it is useful to extract experimental observables to extract useful dynamical information.

Multiplets in the 2nd excitation band of N^*

V. Crede and W. Roberts, Rept.Prog.Phys. **76** (2013)

$SU(6)$ (flavor + spin), $O(3)$: orthogonal group of rotations
$6 \otimes 6 \otimes 6 = 56_S \oplus 70_M \oplus 70_M \oplus 20_A$
$56 = 10^4 \oplus 8^2$, $(4 = 2(\frac{3}{2}) + 1)$
$70 = 10^2 \oplus 8^4 \oplus 8^2 \oplus 1^2$
$20 = 8^2 \oplus 1^4$

Why is 20plet inconsistent with the static quark-diquark picture?
The static diquark: $6 \otimes 6 = 21 \oplus 15$
The symmetry of diquark requires it to be 21 since the color $\Psi$is antisymmetric.
The static diquark +the third quark: $21 \otimes 6 = 56 \oplus 70$, i.e. no 20plet!

Only two N^*states with 1-star rating have been assigned to the 20plet.

Light Baryon Spectroscopy

The **ground state** of light baryons can be grouped in multiplets.

- Baryons with $J^P = \frac{1}{2}^+$ in an octet.
- Baryons with $J^P = \frac{3}{2}^+$ in a decuplet.

All of them have been experimentally observed.

Naming light baryons: Symbol (Mass in MeV/c^2) J^P

- **Baryon with 0 s quark**: N if $I = 1/2$, Δ if $I = 3/2$.
- With 1 s quark: Λ if $I = 0$, Σ if $I = 1$.
- With 2 s quarks: Ξ. It has $I = 1/2$.
- With 3 s quarks: Ω. It has $I = 0$.

Baryon octet

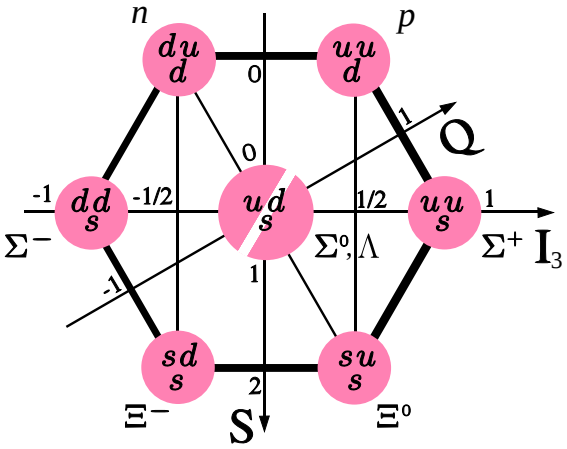

Baryon decuplet

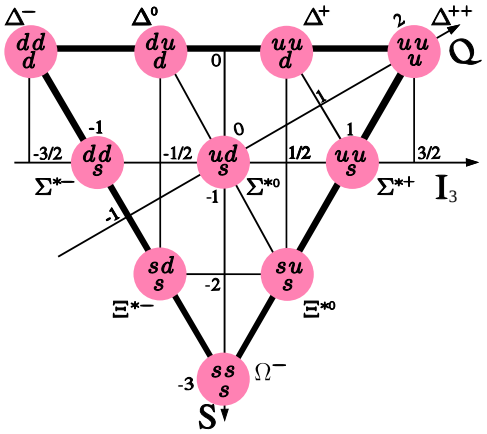

The Unbinned Maximum Likelihood Method (MLM)

- The ϕ_{lab} asymmetry was manifested as modulations.

  E.g. Asymmetry, $A = \frac{N_\omega(\Rightarrow,+) - N_\omega(\Rightarrow,-)}{N_\omega(\Rightarrow,+) + N_\omega(\Rightarrow,-)}$

Data integrated over all kinematic bins.

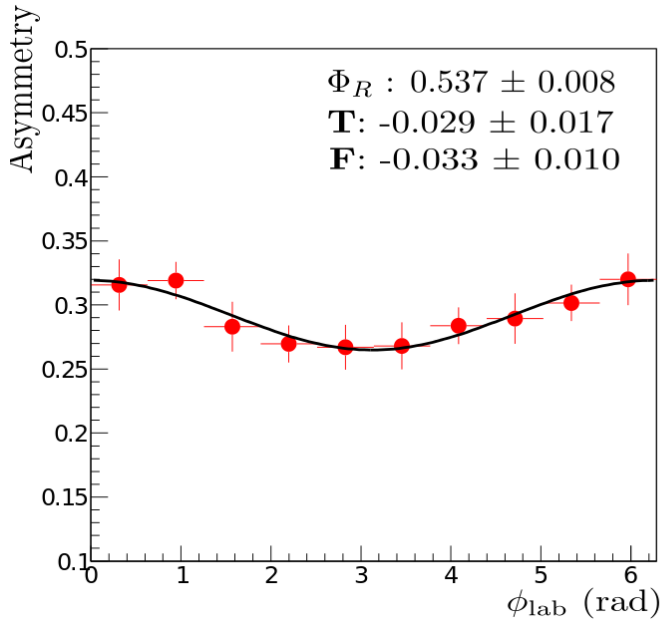

The Unbinned Maximum Likelihood Method (MLM)

- The ϕ_{lab} asymmetry was manifested as modulations.
- Polarization observables were extracted by fitting the modulations using unbinned MLM. **Advantage**: no loss of information due to binning.

$$-\ln L = -\sum_{i=1}^{N_{\text{total}}} w_i \ln\left(P\left(\text{event}_i\right)\right), \; A = \frac{(n_{\text{pol1}} - n_{\text{pol2}})}{(n_{\text{pol1}} + n_{\text{pol2}})},$$

$$\text{where } P\left(\text{event}_i\right) = \begin{cases} \frac{1}{2}(1 + A), & \text{for pol1}, \\ \frac{1}{2}(1 - A), & \text{for pol2 (orthogonal to pol1).} \end{cases}$$

- A was a function of the polarization observable. Minimizing $-\ln L$ gave the most likely value of the observable.

The Unbinned Maximum Likelihood Method (MLM)

- The ϕ_{lab} asymmetry was manifested as modulations.
- Polarization observables were extracted by fitting the modulations using unbinned MLM. **Advantage**: no loss of information due to binning.

$$-\ln L = -\sum_{i=1}^{N_{\text{total}}} w_i \ln\left(P\left(\text{event}_i\right)\right), \; A = \frac{(n_{\text{pol1}} - n_{\text{pol2}})}{(n_{\text{pol1}} + n_{\text{pol2}})},$$

$$\text{where } P\left(\text{event}_i\right) = \begin{cases} \frac{1}{2}(1 + A), & \text{for pol1}, \\ \frac{1}{2}(1 - A), & \text{for pol2 (orthogonal to pol1).} \end{cases}$$

- A was a function of the polarization observable. Minimizing $-\ln L$ gave the most likely value of the observable.

Beam Asymmetry in ω Photoproduction

$$2\,\pi\,W^f(\Phi,\Psi) = 1 - \Sigma^f_\Phi \cos 2\Phi \; - \; P_\gamma\,\Sigma^f_b \cos 2\Psi \; + \; P_\gamma\,\Sigma^f_d \cos 2(\Phi \; - \; \Psi)$$

(A. I. Titov and B. Kampfer, Phys. Rev. C 78, 038201 (2008))

$$\Sigma^h_b \; = \; \Sigma^r_b \; = \; 2\rho^1_{11} \; + \; \rho^1_{00}$$

$$-\tfrac{1}{2}\Sigma^h_d \; = \; \Sigma^r_d \; = \; \rho^1_{1-1}$$

$$-\tfrac{1}{2}\Sigma^h_\Phi \; = \; \Sigma^r_\Phi \; = \; -\rho^0_{1-1}$$

Pol. SDMEs: B. Vernarsky (CMU), PhD dissertation

Ψ : angle between $p\,\omega$ production plane and photon polarization plane in the overall CM frame.

Φ : azimuthal angle of normal to the ω decay plane in helicity frame, quantization axis in the direction opposite the recoling proton in the ω rest frame.

First Measurements of Target Asym. $P_{x,y}$ in $\gamma\vec{p} \to p\pi^+\pi^-$

Example: $0.8 < E_\gamma < 0.9$ GeV (Total E_γ range covered: 0.7 - 2.1 GeV)

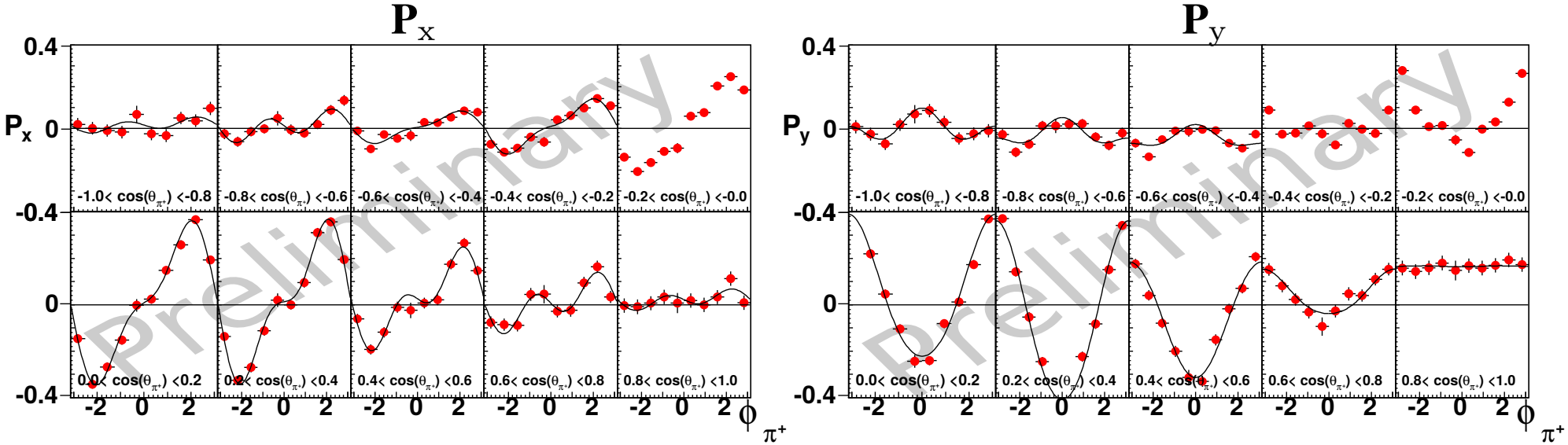

FROST g9b (lin. pol. beam) **Solid curves : Fourier fit ($n < 3$)**

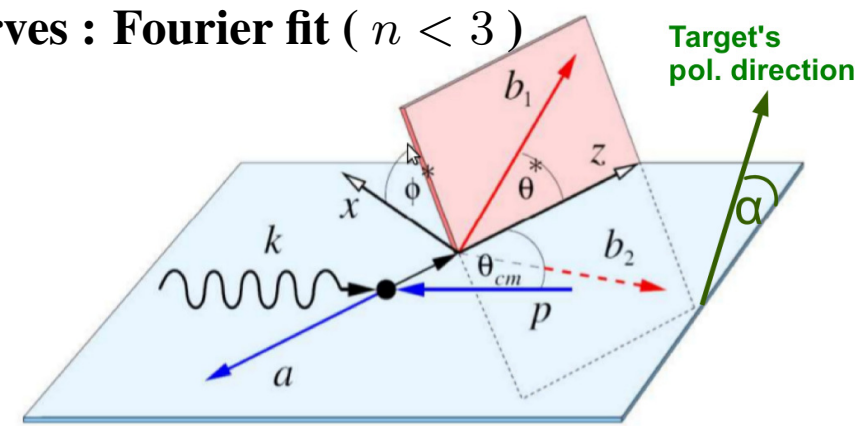

3-dim. phase space: $(E_\gamma, \phi^*_{\pi^+}, \cos\theta^*_{\pi^+})$

$$I = I_0[1 + \Lambda\cos(\alpha)P_x + \Lambda\sin(\alpha)P_y]$$

Λ : degree of target pol.

W. Roberts and T. Oed, PRC **71**, 055201 (2005)

Published Results in $\vec{\gamma}\vec{p} \to p\pi^+\pi^-$

Allow the study of sequential decays of intermediate N^* and also $N^* \to p\rho$ decay but the large hadronic background makes it challenging.

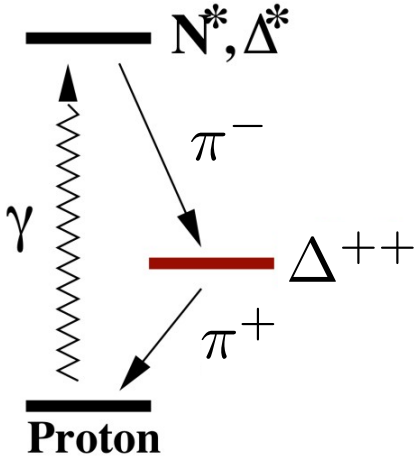

Published Results in $\vec{\gamma}\vec{p} \to p\pi^+\pi^-$

Polarization observables database rather sparse in the past. Moreover, existing models do not describe the data well.

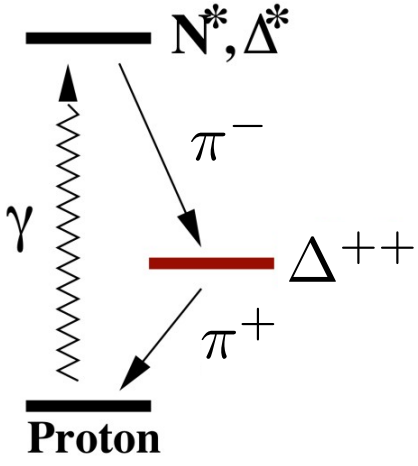

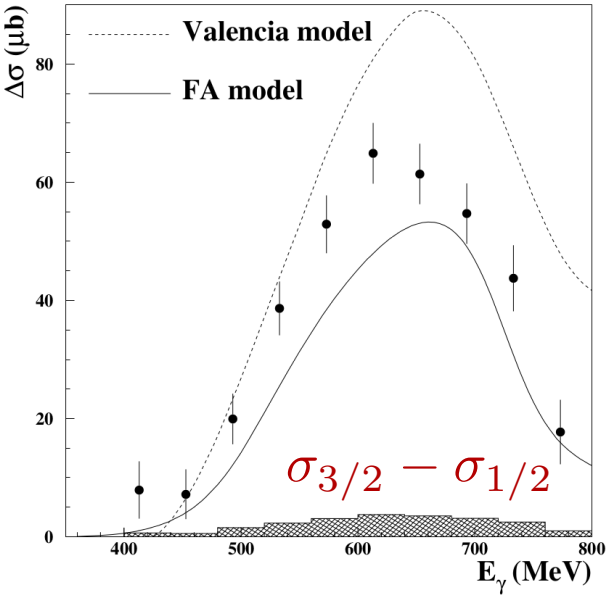

Beam \ Target	Transversely Pol.	Longitudinally Pol.
Linearly Pol.	$P^{s,c}_{x,y}$, $P_{x,y}$, $I^{s,c}$	$P^{s,c}_{z}$, P_{z}, $I^{s,c}$
Circularly Pol.	$P^{\odot}_{x,y}$, $P_{x,y}$, $I^{\odot}$	$P^{\odot}_{z}$, P_{z}, $I^{\odot}$

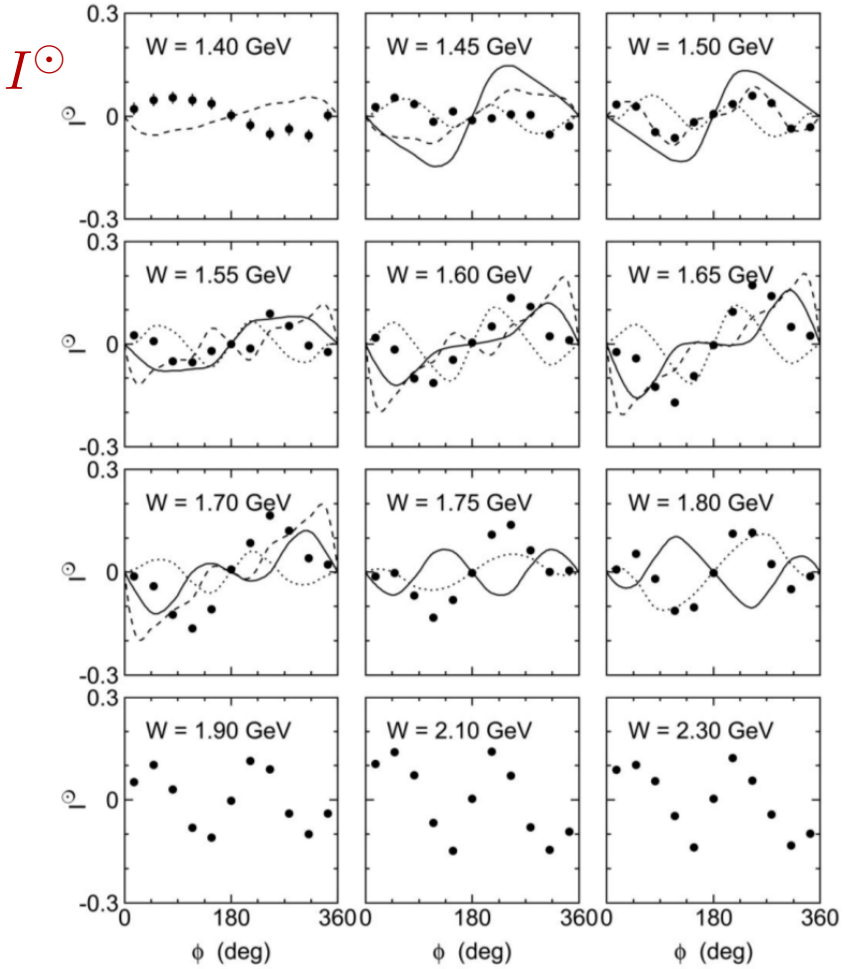

Strauch *et al.*, PRL **95**, 162003 (2005); Krambrich *et al.*, PRL **103**, 052002 (2009)
Ahrens *et al.*, EPJ A **34**, 11 (2007)

First Measurements of P_x^c in $\vec{\gamma}\vec{p} \to p\pi^+\pi^-$

-1.0 < $\cos\theta^*_{\pi^+}$ < 0.0

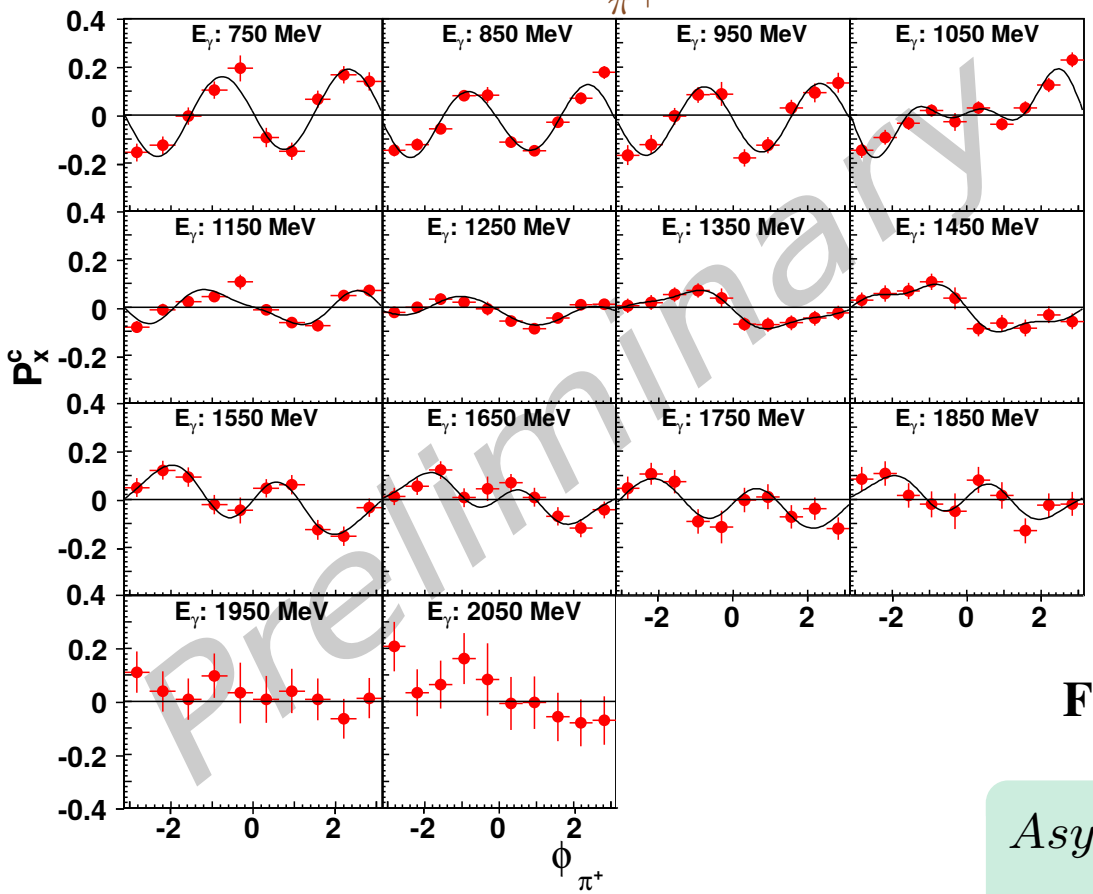

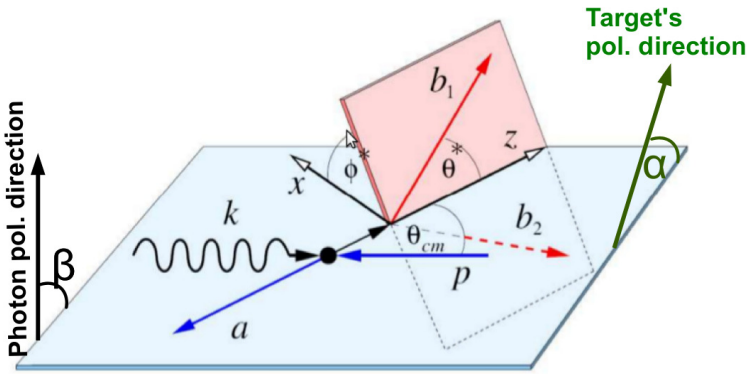

FROST g9b (lin. pol. beam)

Solid Line - Fourier fit ($n < 4$)

Fine binning in (E_γ, $\phi^*_{\pi^+}$), 2 bins in $\cos\theta^*_{\pi^+}$

$$Asym. = \delta_l \Lambda\{\sin 2\beta(\mathbf{P_x^s}\cos\alpha + \mathbf{P_y^s}\sin\alpha) + \cos 2\beta(\mathbf{P_x^c}\cos\alpha + \mathbf{P_y^c}\sin\alpha)\}$$

$\delta_l(\Lambda)$: degree of beam (target) pol.

First Measurements of P_x^c in $\vec{\gamma}\vec{p} \to p\pi^+\pi^-$

$0.0 < \cos\theta^*_{\pi^+} < 1.0$

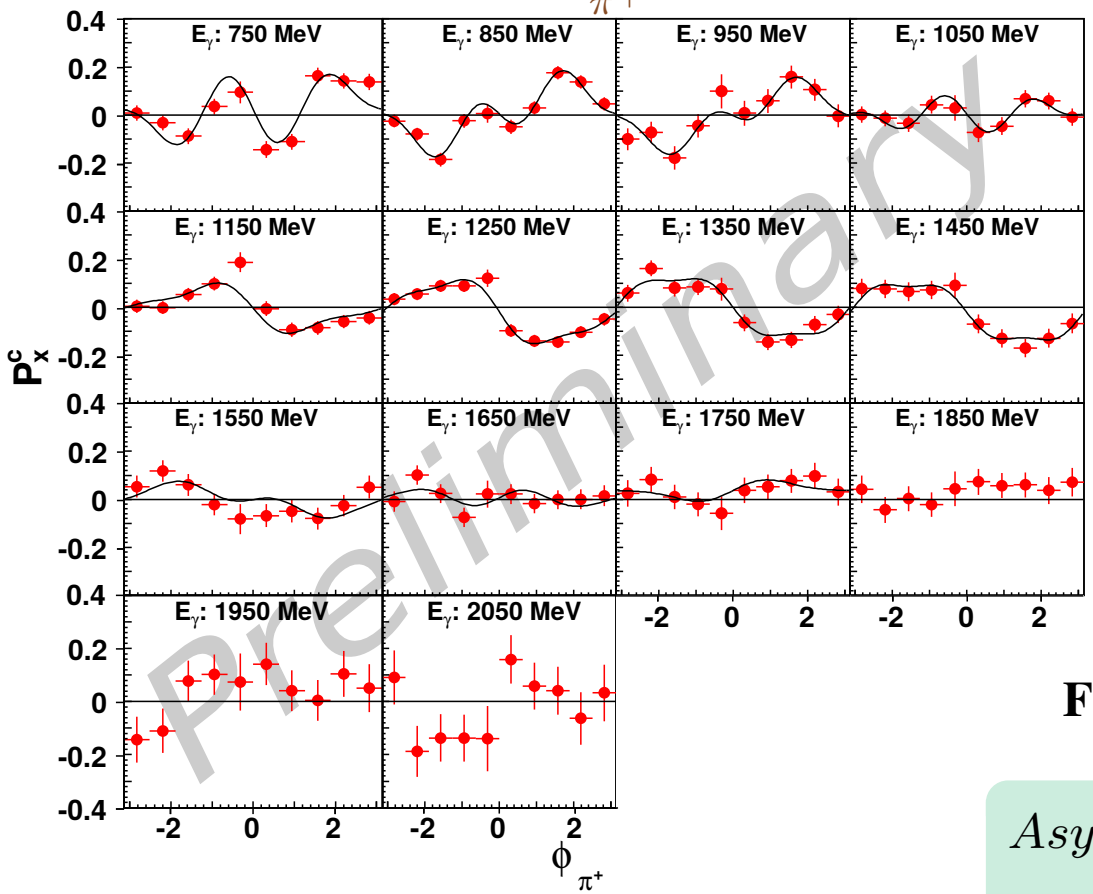

FROST g9b (lin. pol. beam)

Solid Line - Fourier fit ($n < 4$)

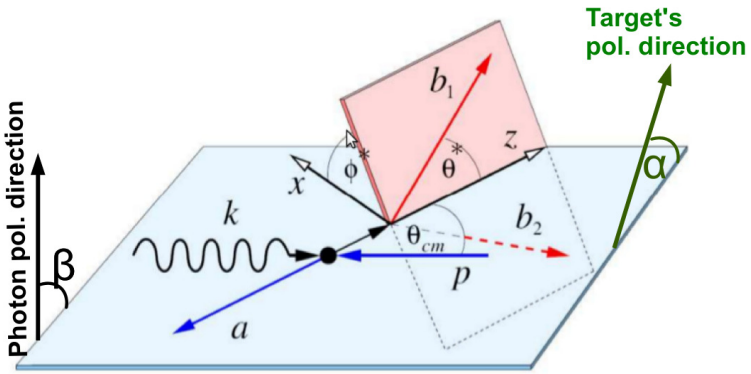

Fine binning in (E_γ, $\phi^*_{\pi^+}$), 2 bins in $\cos\theta^*_{\pi^+}$

$$Asym. = \delta_l \Lambda\{\sin 2\beta(\mathbf{P_x^s}\cos\alpha + \mathbf{P_y^s}\sin\alpha) + \cos 2\beta(\mathbf{P_x^c}\cos\alpha + \mathbf{P_y^c}\sin\alpha)\}$$

$\delta_l(\Lambda)$: degree of beam (target) pol.